

Design and Development of Membrane Electrode Assembly for Proton Exchange

Membrane Fuel Cell

by

Harshal Anil Kasat

A Thesis Presented in Partial Fulfillment
of the Requirements for the Degree
Master of Science

Approved July 2016 by the
Graduate Supervisory Committee:

A.M. Kannan, Co-Chair

Patrick Phelan, Co-Chair

Abdelrahman Shuaib

ARIZONA STATE UNIVERSITY

August 2016

ABSTRACT

This work aimed to characterize and optimize the variables that influence the Gas Diffusion Layer (GDL) preparation using design of experiment (DOE) approach. In the process of GDL preparation, the quantity of carbon support and Teflon were found to have significant influence on the Proton Exchange Membrane Fuel Cell (PEMFC). Characterization methods like surface roughness, wetting characteristics, microstructure surface morphology, pore size distribution, thermal conductivity of GDLs were examined using laser interferometer, Goniometer, SEM, porosimetry and thermal conductivity analyzer respectively. The GDLs were evaluated in single cell PEMFC under various operating conditions of temperature and relative humidity (RH) using air as oxidant. Electrodes were prepared with different PUREBLACK[®] and poly-tetrafluoroethylene (PTFE) content in the diffusion layer and maintaining catalytic layer with a Pt-loading (0.4 mg cm^{-2}). In the study, a 73.16 wt.% level of PB and 34 wt.% level of PTFE was the optimal compositions for GDL at $70 \text{ }^{\circ}\text{C}$ for 70% RH under air atmosphere.

For most electrochemical processes the oxygen reduction is very vital reaction. Pt loading in the electrocatalyst contributes towards the total cost of electrochemical devices. Reducing the Pt loading in electrocatalysts with high efficiency is important for the development of fuel cell technologies. To this end, this thesis work reports the approach to lower down the Pt loading in electrocatalyst based on N-doped carbon nanotubes derived from Zeolitic Imidazolate Frameworks (ZIF-67) for oxygen reduction. This electrocatalyst performs with higher electrocatalytic activity and stability for oxygen reduction in fuel cell testing. The electrochemical properties are mainly due to

the synergistic effect from N-doped carbon nanotubes derived from ZIF and Pt loading. The strategy with low Pt loading forecasts in emerging highly active and less expensive electrocatalysts in electrochemical energy devices.

This thesis focuses on: (i) methods to obtain greater power density by optimizing content of wet-proofing agent (PTFE) and fine-grained, hydrophobic, microporous layer (MPL); (ii) modeling full factorial analysis of PEMFC for evaluation with experimental results and predicting further improvements in performance; (iii) methods to obtain high levels of performance with low Pt loading electrodes based on N-doped carbon nanotubes derived from ZIF-67 and Pt.

DEDICATION

I would like to dedicate this to my parents Anil and Mangala Kasat who ensured that I was provided with every tool required to achieve. They have been there for me my entire life, and their unwavering support has given me the confidence to tackle tough times at Arizona State University. And I would like to thank all my friends, without whom none of my success would be possible. Finally, and most importantly, loving thanks to Harsha C. Pol, for her constant and overflowing support and encouragement.

ACKNOWLEDGMENTS

I would first like to express my sincere thanks to Professor A.M. Kannan for his astounding support and help in this project. He helped me overcome the difficulties I faced during the entire project. His willingness to help me every time I encountered an issue helped me a lot to get through with this project. Without his guidance and profound help, it would not have been possible for me to complete this project. In addition, I would like to thank Professor Patrick Phelan, Professor Abdelrehman Shuaib who obliged me with being part of my committee.

I would also like to thank my lab mate in Dr. Kannan's research group: Brahim Laoun for helping me out with my project, giving me useful suggestions that helped me complete the project successfully.

I would also like to express my gratitude to Mr. Riaz Ahmad from Quantachrome Instruments for pore size distribution measurements which was a crucial result of this report.

TABLE OF CONTENTS

	Page
LIST OF TABLES.....	viii
LIST OF FIGURES.....	ix
CHAPTER	
1 INTRODUCTION	1
1.1 Background and Motivation	1
1.2 Proton Exchange Membrane Fuel Cells (PEMFC).....	4
1.3 Gas Diffusion Layer	5
1.3.1 Carbon Support Material	7
1.4 Proton Exchange Membranes	9
1.4.1 Catalyst Layer	10
1.5 Problem Statement.....	11
1.6 Organization of the Thesis.....	14
2 LITERATURE REVIEW	16
2.1 Datta Et. Al. Paper on Understanding of GDL in PEMFC	16
2.2 Kannan Et. Al. Review of Characterization Techniques for GDL for PEMFC..	18
2.2.1 Thermal Conductivity.....	18
2.2.2 Porosity and Pore Size Distribution.....	19
2.2.3 Surface Morphology.....	19
2.2.4 Contact Angle.....	20

CHAPTER	Page
2.3 Kannan Et. Al. Paper on GDL Using New Type of Graphitized Nano-Carbon Pureblack [®] for PEMFC.....	20
2.4 Kannan Et. Al. Paper on Effect of Carbon Substrate of GDL on Performance of PEMFC	20
2.5 Kannan Et. Al. Paper on Wire Rod Coating Process of Gas Diffusion Layer for PEMFCS	21
2.6 Lim Et. Al. Paper on Effects of Hydrophobic Polymer Content in GDL on Power Performance of a PEM Fuel Cell.....	22
2.7 Kannan Et. Al. Paper on Development of GDL Using Water Based Carbon Slurry for PEMFC	23
2.8 Cho Et. Al. Paper on Optimization of GDLs for High Performance PEMFC Employing Stainless Steel Bipolar Plates	23
2.9 Xia Et. Al. Paper on MOF Derived Bifunctional Oxygen Electrocatalyst.....	25
3 METHODOLOGY	27
3.1 Experimental Protocol for Gdl Optimization	27
3.1.1 Gas Diffusion Layer	27
3.1.2 Catalyst Coated Membrane.....	30
3.1.3 Fuel Cell Assembly and Testing.....	31
3.2 Experimental Protocol for PT-NCNTFS Cathode Catalyst Using ZIF-67.....	33
3.2.1 Gas Diffusion Layer	33
3.2.2 Catalyst Coated Membrane.....	35

CHAPTER	Page
3.2.3 Fuel Cell Assembly and Testing.....	36
4 RESULTS AND DISCUSSION.....	38
4.1 GDL Optimization.....	38
4.2 PT-NCNTFS Cathode Catalyst Using ZIF-67.....	46
5 CONCLUSION.....	51
6 REFERENCES.....	53

LIST OF TABLES

Table	Page
1 Physico-Chemical Properties of PUREBLACK [®] 205-110 Carbon.....	8
2 Values of Various Individual Parameters at Two Levels	30
3 2 ² -Factorial Design: GDL Samples Were Fabricated with Following Different Concentration of PB and PTFE.....	30
4 Fuel Cell Performance Data of MEA with Various GDL Compositions	39
5 Final Design of GDL	40

LIST OF FIGURES

Figure	Page
1 Observed Changes in (a) Global Average Surface Temperature, (b) Global Average Sea Level from Tide Gauge (Blue) and Satellite (Orange) Data and (c) Northern Hemisphere Snow Cover.....	2
2 Schematic of a PEM Fuel Cell.....	5
3 Carbon Paper with Microporous Layer.....	6
4 Schematic Representation of Micelle-Encapsulated PUREBLACK [®] and VGCF Carbons	9
5 Primary Chemical Structure of Nafion	10
6 Water Management in PEMFC.....	12
7 Process of Coating Carbon Paper with Microporous Layer	28
8 Design of Experiments Approach.....	29
9 CCM Micro-Spray Method.....	31
10 Greenlight Test Station (G50 Fuel Cell System, Hydrogenics, and Vancouver, Canada)	33
11 Easycaoter Equipment (EC26, Coatema) Used for Coating GDL.....	34
12 Synthesis of Pt-NCNTFs Using ZIF-67.....	36
13 Fuel Cell Performance Using Various Content of PB and PTFE in GDL at 70 °C with H ₂ and Air Gases, 70 % RH. The Open Symbols Are the Power Density Values	39
14 Fuel Cell Performance of Optimized GDL at 70 °C with H ₂ and Air Gases, 70 % RH. The Open Symbols Are the Power Density Values	40

Figure	Page
15 (a) Specific and (b) Cumulative Pore-Size Distribution of Diffusion Layer from Mercury-Intrusion Porosimetry Measurements	41
16 Contact Angle Images of (a) GDL#1 (b) GDL#2 (c) GDL#3 (d) GDL#4	43
17 Wetting Angle Images of (a) Optimized GDL#1 (b) Optimized GDL#2.....	44
18 Scanning Electron Micrographs of Surface of Optimized Diffusion Layer #2 at (a) 25x (b) 1000x.....	45
19 Scanning Electron Micrographs of (a,b) Pt-NCNTFs, and Transmission Electron Micrographs of (c) NCNTFs and (d) Pt-NCNTFs.....	47
20 X-Ray Diffractograms of (a) NCNTFs and (b) Pt-NCNTFs.....	49
21 Fuel Cell Performance using Pt-NCNTFs Cathode Catalysts at Various Temperatures with H ₂ and O ₂ gases, 100 % RH. The Open Symbols are the Power Density Values	50

ABBREVIATIONS

GHG: Green House Gas

IPCC: Intergovernmental Panel on Climate Change

PEMFC: Proton Exchange Membrane Fuel Cell/ Polymer Electrolyte Membrane Fuel Cell

GDL: Gas Diffusion Layer

MEA: Membrane Electrode Assembly

CCM: Catalyst coated membrane

MPL: Micro-porous Layer

CL: Catalyst Layer

CFP: Carbon Fiber Paper

PB: PUREBLACK[®]

VGCF: Vapor grown carbon fiber

SDS: Sodium Dodecyl Sulfate

ORR: Oxygen reduction reactions

DOE: Design of Experiments

SCCM: Standardized cubic centimeters per minute

MOF: Metal organic frameworks

ZIF: Zeolitic imidazolate frameworks

NCNTF: Nitrogen doped Carbon Nanotube framework

DI water: Deionized water

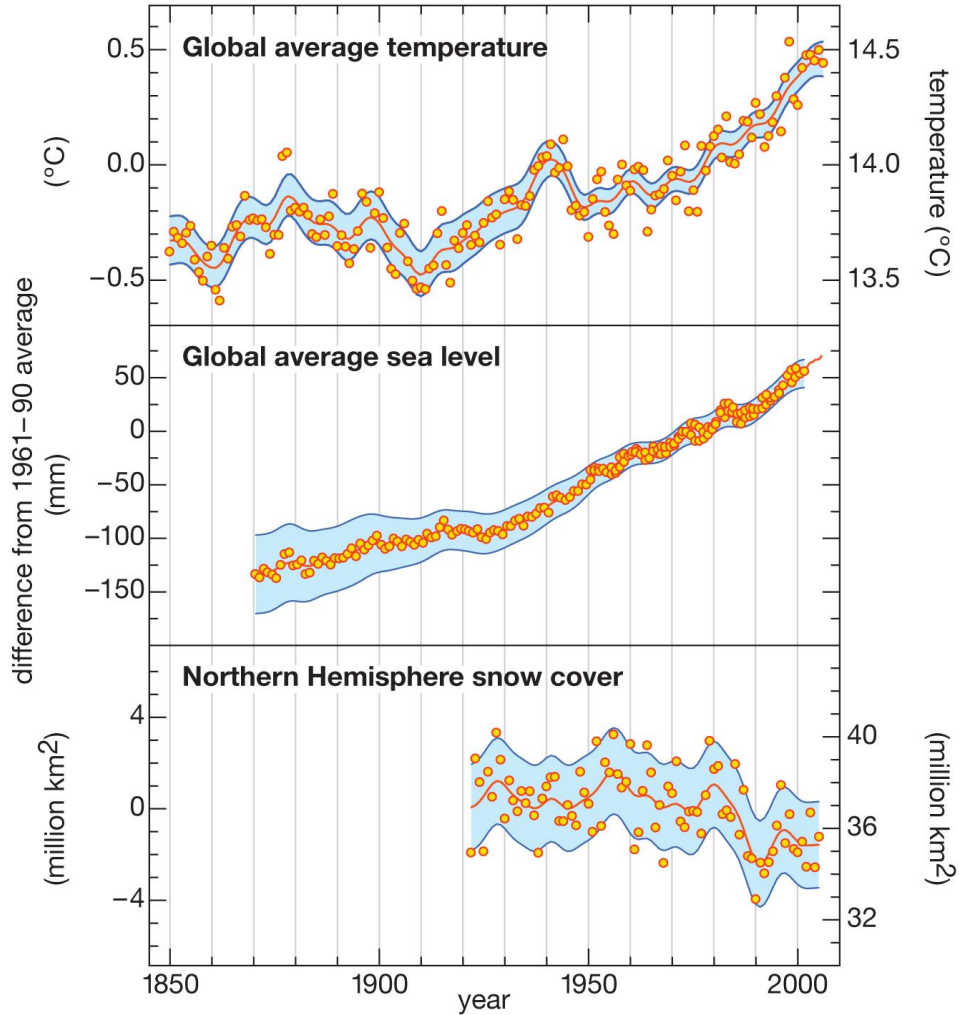
IPA: Isopropyl alcohol

1 INTRODUCTION

1.1 BACKGROUND AND MOTIVATION

Since decades, fossil fuels, especially petroleum has been the primary energy source for conveyance. Though it has been a cheaper and better performing alternative than other fuels in the past, recent years have observed a trend towards using alternative and sustainable sources of energy in transportation sector. The reasons behind this shift are the non-renewable nature of fossil fuel, increasing cost of petroleum products, as well as the environmental threats due to the generation of greenhouse gases (GHG), contributing towards global warming more than ever. In 2012, 1.17 billion barrels of petroleum products were consumed in the US[1], which contributed to a 5.026×10^9 tons of greenhouse gases released into the atmosphere[2]. CO₂ being the most salient GHG. The global atmospheric concentration of CO₂ has increased from a pre-industrial value of about 280 to 379 parts per million in 2005[3]. Warming of the climate system is unequivocal. This can be found in evidence of increases in global average air and ocean temperatures, widespread melting of snow and ice, and rising sea levels.

As shown in *Figure 1*, the Intergovernmental Panel on Climate Change (IPCC) assessment builds that during the second half of the 20th century and early part of the 21st century, global average surface temperature increased due to observed increase in anthropogenic greenhouse gas (GHG) concentrations. Mountain glaciers and snow cover have declined contributing to sea level rise at an average rate of 1.8 mm per year from 1961 to 2003. Again over the same period, the amount of snow cover in the Northern Hemisphere decreased.



Source: Climate Change 2007: The Physical Science Basis, Summary for Policymakers, Intergovernmental Panel on Climate Change

Figure 1 Observed Changes in (a) Global Average Surface Temperature, (b) Global Average Sea Level from Tide Gauge (Blue) and Satellite (Orange) Data and (c) Northern Hemisphere Snow Cover

To address all these legislations and to comply with standards like Corporate Average Fuel Economy (CAFÉ) as well as California zero-emission vehicle, there is an increasing pressure on automotive manufacturers to produce more efficient and alternative fuel vehicles. With the depletion of fossil fuels and growing concerns over environmental issues such as global warming, there has been a keen interest in research related to fuel cells.

Fuel cell combines the advantage of both combustion engine as well as a battery except for the fact that fuel cells can be operated continuously as long as it is provided with the required amount of fuel and oxidant. Fuel cells (particularly hydrogen) due to their high efficiency and zero pollution provide the promise of being one of the long-term solutions to the improvement of energy efficiency, energy sustainability, and energy security and the reduction of greenhouse gases and urban pollution. The use of hydrogen as fuel will greatly reduce the polluting CO and NO_x emissions.

PEMFCs have the potential to become both reliable and commercial energy generators in the near future. But the key challenges currently hampering widespread Proton Exchange Membrane Fuel Cell (PEMFC) commercialization are their high costs and limited hydrogen availability[4]. Subsequently fuel cell material costs is directly proportional with active area, thus the key to reducing the costs is to enable greater power densities from PEM fuel cells, so that compact fuel cell configurations can handle greater power ranges[5]. As power densities increase, heat transfer and gas diffusion rates become limiting factors to performance, and both of these factors are heavily influenced by the porous transport layer which is referred to as the gas diffusion layer (GDL)[6, 7].

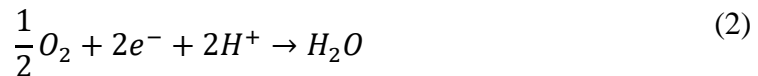
1.2 PROTON EXCHANGE MEMBRANE FUEL CELLS (PEMFC)

Polymer electrolyte fuel cells gained momentum due to the low operating temperature (<100 °C), attainable high power densities, fast start-up capability and their relatively simple handling. This fuel cell utilizes ionically conductive polymer usually perfluorosulfonic acid (Nafion) membrane which acts as electrolyte; impermeable to gases but it conducts protons. The membrane that acts as the electrolyte is sandwiched between the two porous, electrically conductive electrodes. These electrodes are typically made out of carbon cloth or carbon fiber paper. At the interface between the porous electrode and the polymer membrane there is a layer with catalyst particles, typically platinum supported on carbon (see Fig. 1.2). The composite structure of gas diffusion layer, anode, proton exchange membrane, cathode and gas diffusion layer is known as membrane electrode assembly (MEA). Oxygen from air and hydrogen fuel are channeled to the cathode and anode side, respectively through flow channels (Bipolar plates).

The hydrogen molecule is ionized on the anode side:



and its product species protons and electrons are recombined with an oxygen atom to produce a water molecule on the cathode side:



The hydrogen ion permeates through ionomer membrane and reaches cathode side; however, the electrons are routed around an external circuit, providing useful electricity.

The migration of proton in membrane is promoted by sulphonate group present in the membrane structure through the formation of hydronium ion.

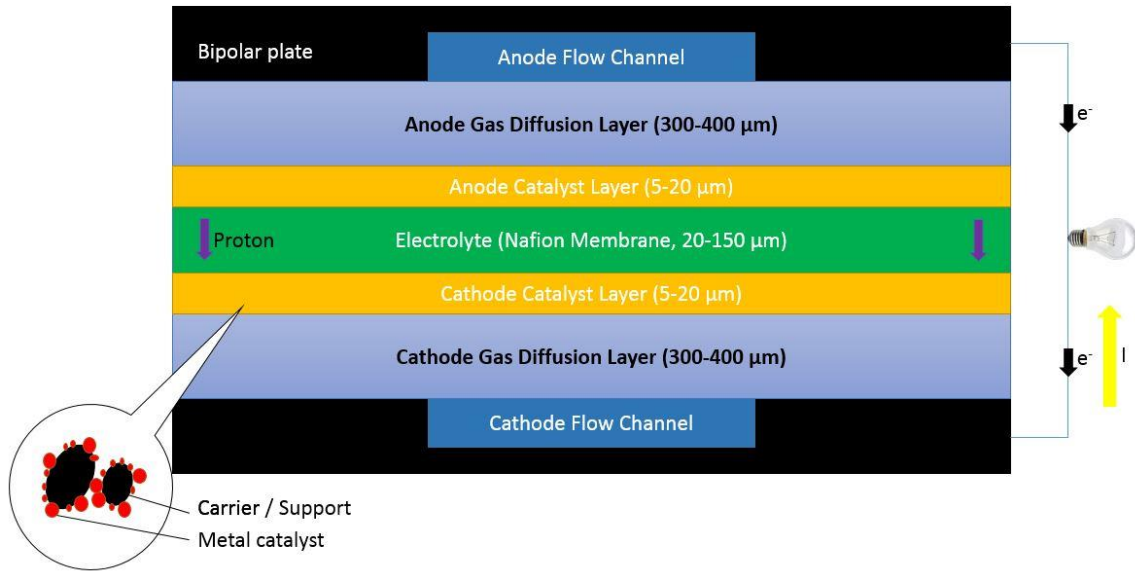


Figure 2 Schematic of a PEM Fuel Cell

1.3 GAS DIFFUSION LAYER

The macro-porous layer of diffusion layer (DL) is either carbon paper or woven carbon cloth which serves as physical substrate for catalyst layer, current collector as well as an elastic component of the MEA. The DL are fabricated using carbon paper in a PEMFC are usually treated (coated) with a hydrophobic agent such as PTFE in order to improve the water removal within the DL and the fuel cell. It is also very common to have a catalyst-backing layer or microporous layer (MPL) between the catalyst layer (CL) and diffusion layer. The MPL consists of thin layer of carbon black mixed with PTFE coated on to a sheet of macro-porous carbon fiber paper (CFP), due to their high porosity ($\geq 70\%$) and good electrical conductivity.



Figure 3 Carbon Paper with Microporous Layer

GDL is a vital component of MEA and fuel cell because it provides the following functions and properties:

- a) Maintain water balance in MEA by allowing removal of water produced and accumulated in the CLs toward the flow field channels. The DL must have large enough pores so that the condensed water can leave the CL, MPL, and DL without blocking any pores that may affect the transport of reactant gases or liquids[8, 9].

- b) It provides mechanical support to the CL and the membrane in order for these two components to be unaffected by the pressure that the landings or ribs of the bipolar plate put on them. Thus the DL should not deform substantially after several hours of operations [10, 11].
- c) It helps to provide electrical contact from the bipolar plates to the CL and vice versa with low resistance between them[12].
- d) It also helps in heat transfer from CL to the bipolar plates in order to keep the cell at desired temperature of operation[13].

1.3.1 CARBON SUPPORT MATERIAL

The micro-porous layer of gas diffusion layers (GDLs) was fabricated with the PUREBLACK[®] carbon powder along with vapor grown carbon fiber (VGCF) dispersed in sodium dodecyl sulfate (SDS) aqueous solvent mixed with polymeric binder (usually PTFE). Microporous layers have a pore size between 100 and 500 nm, as compared with 10–30 μ m pore size for carbon-fiber-paper substrates[14].

Carbon powder is used as support material for the following reasons

- a) Availability of variable surface area and porosity.
- b) High electrical and thermal conductivity.
- c) Stable in reducing and reasonably oxidizing environments.

Carbon powder characteristics affects the linear as well as non-linear polarization components as well as reversible potential of the cell (E°). Carbon support should have a higher surface area as it increases the oxidation.

PUREBLACK[®] has inherent hydrophobic characteristics which leads to relatively better gas transport as well as water management characteristics especially at high current densities, in 100% RH operation. *Table 1* lists the physico-chemical properties of PUREBLACK[®] 205-110 Carbon

Table 1: Physico-Chemical Properties of PUREBLACK[®] 205-110 Carbon

Property	Surface Area (m ² /g)	Moisture (ppm)	Sulphur (ppm)	Volatile matter (%)	Particle size (nm)	Ash (ppm)
PUREBLACK [®]	46	20	<50	0.03	44	20

VGCF is mixed with nano-chain Pureblack[®] 205-110 to offer adhesion and increased mechanical strength between macro-porous and micro-porous layers. Also, the robustness of the micro-porous layer was improved by combining PUREBLACK[®] carbon with a fibrous nano-carbon.

As shown in *Figure 4*, SDS molecules are chemically adsorbed on the surface of the carbon particles, forming micelle-encapsulation [15]. The SDS, anionic surfactant is attached to the surface of carbon particle/fiber assisting homogenous dispersion of the slurry in water medium. GDLs fabricated using SDS water solution as a medium of dispersion for carbon slurry has been found to be better performer compared to GDLs fabricated with alcohol based solution[16].

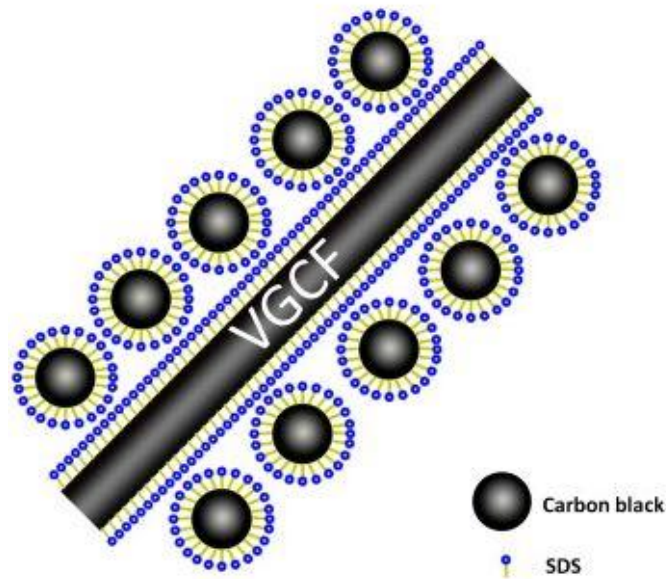


Figure 4 Schematic Representation of Micelle-Encapsulated PUREBLACK[®] and VGCF Carbons

1.4 PROTON EXCHANGE MEMBRANES

Effective proton exchange membrane should possess the following properties:

- a) High proton conductivity
- b) Possess high thermomechanical and chemical stability
- c) Impermeable to gases (oxygen) and fuels (hydrogen)
- d) Achieve balanced water transport

Nafion which is a perfluorosulphonic polymer electrolyte (see *Figure 5*) has been durable over long time up to 60,000 h; since they can withstand harsh chemical and physical environment in PEMFC[17]. Protons on the sulfonic acid group (SO₃H) “hop” from one acid site to another. The pores thus allow movement of cations but the membranes do not

conduct anions. Depending on temperature and hydration state the proton conductivity may be up to 0.2 S/cm.

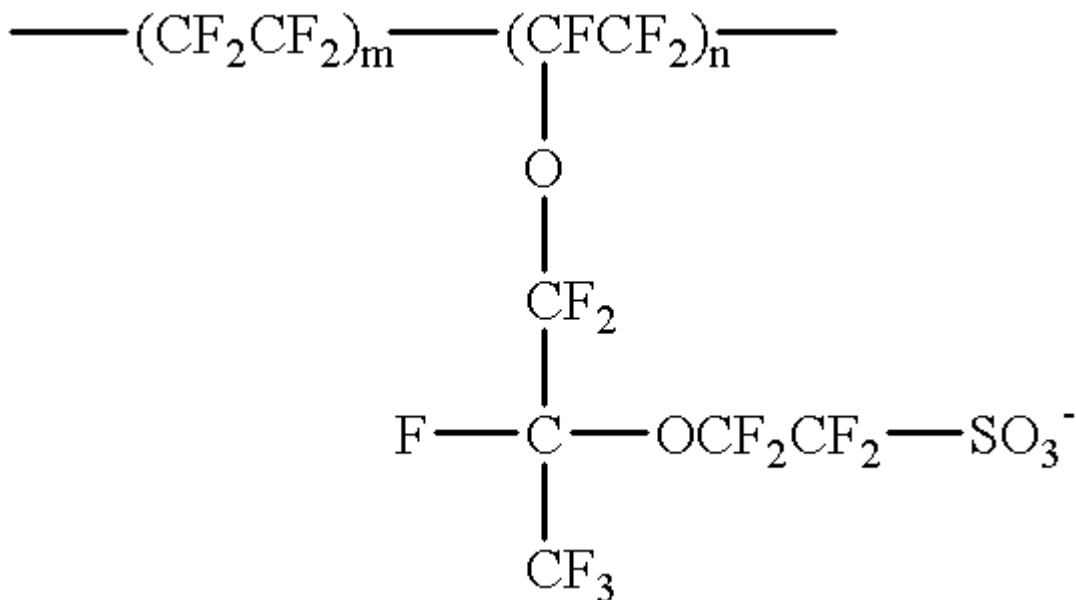


Figure 5 Primary Chemical Structure of Nafion

1.4.1 CATALYST LAYER

Oxygen reduction reactions (ORR) is the most important reactions for electrochemical energy conversion and storage technologies, especially fuel cells[18, 19]. Catalyst ink can be applied directly onto the proton exchange membrane to form a catalyst coated membrane (CCM). Conventional CCM is based on Pt/Nafion mixture. Noble metals like platinum (Pt)-based nanocomposites are the most efficient commercial electrocatalysts for the ORR. However noble metal-based oxygen electrocatalysts have high cost, poor stability and scarcity, which are the barriers for the commercial applications of these technologies [20, 21].

Zeolitic imidazolate frameworks (ZIFs) as a subclass of Metal Organic Frameworks (MOF) are excellent materials for the synthesis of nanocarbon electrocatalysts with

abundant carbon and nitrogen [22, 23]. MOF-derived nanocomposites reported as poor ion and electron transport materials due to poor graphitic degree and microporous structures [24-26]. The use of ZIFs as a precursor for the synthesis of N-doped CNTs (NCNTs) structures has rarely been reported for application as electrocatalyst [27-29]. Herein, we report the ultra-low loading of Pt on N-doped carbon nanotube frameworks (Pt-NCNTFs) derived from ZIFs with as an active and stable electrocatalyst for the ORR.

1.5 PROBLEM STATEMENT

The liquid water balance needs to be carefully controlled. The gas diffusion layer provides electrical and thermal conductivity and removes the liquid water. And the proton conductive membrane needs to be hydrated. Water is produced in the catalyst layer of the cathode side.

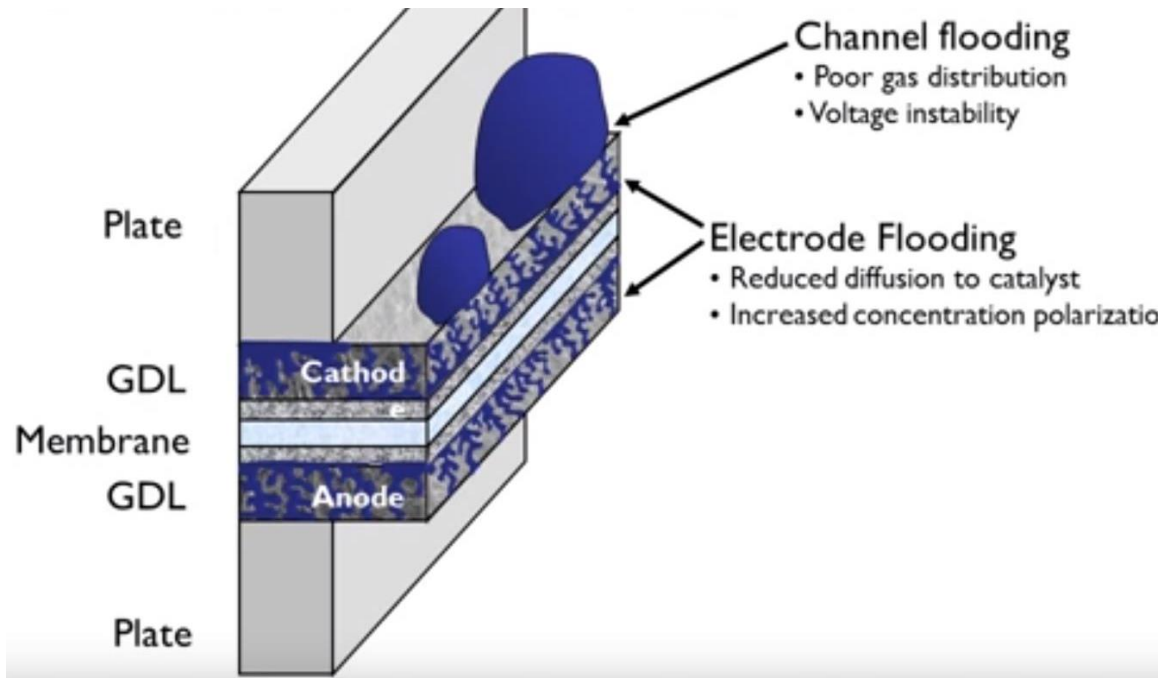


Figure 6 Water Management in PEMFC

If membrane is “too dry” you will not be able to get as much voltage of a fuel cell because ohmic resistance starts going up. Insufficient amount of water in the fuel cell would lead to a higher membrane resistance and membrane dry out, resulting in premature failure of the fuel cell. Thus the membrane needs high humidity for conductivity.

At the same time, excess water in the fuel cell would cause an increase in the mass transport loss at the cathode side resulting in cell degradation. Hence, the desired objective of a water management scheme is to maintain a correct water balance in the fuel cell. In fuel cell flooding the first thing that happens is that the membrane itself is a little bit dry, as you start running some current through here, it starts producing water and the first thing that will happen is that the electrodes themselves will start flooding and then if you

continue to create current faster than you can get water out of the system you will start forming water droplet in the channels. And then you can eventually get to a point where you are producing so much water that the channels themselves are completely flood, completely blocking the ability of oxygen to get to the cathode and that would be one of the reasons that your voltage will quickly start dropping. And that is form of mass transfer over potential. What happens is oxygen cannot get to the electrode fast enough.

The gas diffusion layer is a paper made of carbon fibers with a hydrophobic coating, typically PTFE. In a fully hydrophobic material, water uses the lowest resistance path, which is tortuous. The remaining gas pathways are also tortuous, which leads to transport losses. Air has a double duty, it basically provides oxygen to the electrode and then you need pressure from the air to force out water, so that it does not build up in channels. The GDL is often coated with teflon to shed liquid water and make it hydrophobic. So you don't have droplets of water, that keeps water more in the gaseous phase as it leaves.

Previous studies have demonstrated that metal–organic frameworks (MOFs) with their unique porous structure can act as both templates and precursors for the preparation of porous carbon materials. morphology and crystallinity of carbon materials can be controlled by varying the morphology and metal ions of MOFs. Zeolitic imidazolate frameworks (ZIFs) as an important branch of MOFs are synthesized by coordinating transition metals (Zn^{2+} , Co^{2+}) with imidazole ligands. Thus, ZIFs, which are rich in carbon, nitrogen and transition metals, easily prepared and very cost effective, could be ideal solid-phase precursors for the synthesis of nitrogen-doped carbon materials.

The focal point of this research work is primarily on the proton exchange membrane fuel cell. This thesis will entail and achieve the following objectives:

- a) Fabrication of GDL for optimizing the composition of MPL at 70 °C for 70% RH using air as an oxidant. The durability difficulties of PEMFC becomes especially severe under low humidity and high temperature, which are the desired operation conditions for PEMFC.
- b) Pt-NCNTFs cathode catalyst using ZIF-67 for PEMFC.

1.6 ORGANIZATION OF THE THESIS

This thesis is organized to provide an in-depth understanding of the research work accomplished.

- a) Chapter One gives an introduction to the thesis including background information and the scope of the proposed work.
- b) Chapter Two entails a comprehensive literature review of PEMFC technology: the historical highlights of PEMFC, the technical challenges facing the technology, fabrication of GDLs, and other valuable research work achieved that are significant to this thesis.
- c) Chapter Three describes the experimental procedures and settings to prepare gas diffusion layer. Also, the development and characterization of the different materials for GDLs.
- d) Chapter Four discusses the results of this thesis research by implementing various tools such as PEMFC test, pore size distribution, wetting angle test, SEM and thermal conductivity to evaluate the characterization of GDLs. It also highlights

various tools such as PEMFC test, XRD tests, SEM and TEM to evaluate the characterization of Pt-NCNTFs.

- e) Chapter Five presents the summary and conclusion of the research performed in this thesis. In addition, it also provides the recommendations for future research.

An extensive literature review is done to investigate the effects of varying the compositions of chemicals in GDL to allow further optimization studies. Furthermore, the different range of chemical compositions for namely PB and PTFE are reviewed to select the most suitable range to be evaluated using full factorial design of experiments (DOE). Also, previous works done to analyze the water distribution in fuel cells and to correlate this water accumulation to performance are reviewed. Due to high fuel cell performance loaded catalyst derived by MOF/ZIF reported in recent years, previous works are reviewed. In this chapter, a literature review is provided for

- (i) The techniques that have been applied to fabricate the GDL
- (ii) The impact of different compositions of PB and PTFE on the fuel cell performance
- (iii) The application of ZIF-MOF as the best potential precursor of electrocatalyst due to high surface area of ZIF-MOF morphology, rich in metal ions, presence of carbon and nitrogen in the ligand.

2.1 DATTA ET. AL. PAPER ON UNDERSTANDING OF GDL IN PEMFC

Like previous article, this paper proposes a discussion about influence of structure and design of GDL and MPL on the performance of PEMFC. The objective is to find correlation between ex-situ measured effective diffusivity of water vapor and in-situ performance and limiting current density in PEMFC [30]. The effect of adding multiple MPLs, MPL loading and MPL particle size on cell performance are also investigated. Carbon fiber papers provided by AvCarb Material Solutions were used for this work, since

woven fabrics are ten-folds expensive at high volume production. This paper discusses key GDL structural properties namely thickness, porosity, and pore size distribution. Results show that thicker GDL (>100 microns) show higher total pore volume (4.9 mLg^{-1}) and larger mean pore diameter ($54 \mu\text{m}$) thus making it preferable for wet conditions (>70% RH) as compared to thinner GDL having total pore volume (2.9 mLg^{-1}) and mean pore diameter ($39 \mu\text{m}$) being preferred for low current density/ dry conditions (<30% RH). It was found that at operating conditions of $70 \text{ }^\circ\text{C}$, 12 psig, 2X stoichiometric flows, and 100% RH A/C the fuel cell performance and limiting current was directly proportional until certain value of measured effective water vapor diffusivity. Although two-layer MPL provides higher current density, single MPL serves well for lower power and humidification applications. Lower MPL ($\leq 10 \text{ gm}^{-2}$) loading and medium to small particle size ($5\text{-}20 \mu\text{m}$) led to better fuel cell performance under wet conditions while MPL loading from 10 gm^{-2} to 30 gm^{-2} , medium size particles i.e., $17 \mu\text{m}$, medium thickness and medium PTFE loadings exhibiting better performance under dry conditions.

Morgan et al. [30] identified the role of the GDL and summarized five key features that link the required GDL properties and the best performance of the PEMFC, as follows:

(1) Reactant permeability: The GDL should be macroporous to ensure an efficient supply of reactants (O_2/H_2) to the catalyst layer.

(2) Product permeability: a high product permeability with a balanced water flow in the membrane electrode assembly (MEA) is required. The GDL should prevent the blockage of the catalysts site and prevent the membrane drying [31].

(3) Electrical conductivity: The GDL should ensure a high electrical conductivity to minimize Ohmic losses. In addition, as reported by Morgan et al. the addition of PTFE that increase the porosity reduce the electrical conductivity, thus an optimized PTFE content is required.

(4) Thermal conductivity: an enhanced thermal management is required to remove the heat from the membrane electrode assembly (MEA).

(5) Mechanical support: a robust mechanical support to protect the membrane and catalyst layers from damage during assembly is required from the GDL.

2.2 KANNAN ET. AL. REVIEW OF CHARACTERIZATION TECHNIQUES FOR GDL FOR PEMFC

Various characteristics for GDL has been reviewed including surface morphology, pore size distribution, wettability, thermal and electrical conductivity to achieve optimum fuel cell performance [32]. The method discussed offer understanding which are suitable for large scale as well as small production of GDL materials. Few of the characterization tools are described below:

2.2.1 THERMAL CONDUCTIVITY

Through-plane thermal conductivity measurement setup follows standardized method namely ASTM standard E2584-07 (Standard Practice for Thermal Conductivity of Materials Using a Thermal Capacitance (Slug) Calorimeter) which was succeeded by ASTM E2584-10, ASTM standard D5470-06 (2011) (Standard Test Method for Thermal

Transmission Properties of Thermally Conductive Electrical Insulation Materials). The setup usually consisted of GDL sample compressed between two graphite rods with load range from 0.07-1.38 MPa with the help of loading clamp. Heat flux from the lower rod consisting of a heating element was transmitted to the upper rod. Thermocouples are positioned on lower as well as upper graphite rod at various locations radially to measure the hot side and cold side temperatures of the sample, respectively. The entire system was monitored using Data Acquisition system (DAQ) [33]. The system used to measure the thermal conductivity of GDL as a function of temperature and compression.

2.2.2 POROSITY AND PORE SIZE DISTRIBUTION

Mercury intrusion porosimetry instruments like Quantachrome PoreMaster-33 and Micromeritics AutoPore IV-9500 are majorly used to determine porosity and pore size distribution for GDL. In this method, mercury (Hg) with high surface tension is forced into sample. The pore size distribution divided into micro, meso- and macropores is calculated by the uptake of mercury as a function of pressure using Washburn equation. From total uptake of mercury at the maximum applied pressure, the porosity can be calculated.

2.2.3 SURFACE MORPHOLOGY

GDL surface morphology can be understood using characterization tools such as Scanning electron microscopy (SEM), atomic force microscope (AFM) and laser profilometer. The images captured using above mentioned tools can provide important information regarding mechanical properties of MPL, distribution of adhesion forces and conductive area, average material surface roughness.

2.2.4 CONTACT ANGLE

Sessile drop method is the most frequently used method for measuring the contact angle on diffusion-media surface. Contact angle is an important parameter in PEMFC to regulate the water management. In this method small water droplet ($\leq 1\text{mm}$) is set on the surface and contact angle is measured by fitting tangent to three-phase point where liquid surface and solid surface come in contact. The contact angle can be measured directly by digitizing the image and using a computer program. The wetting characteristics of GDL samples are generally analyzed by Goniometer using water drop.

2.3 KANNAN ET. AL. PAPER ON GDL USING NEW TYPE OF GRAPHITIZED NANO-CARBON PUREBLACK[®] FOR PEMFC

The literature review coins use of a new Nano-carbon material called PUREBLACK[®] as MPL in GDL for PEMFC [35]. The GDL fabricated using PUREBLACK[®] and VGCF performed excellent when air was used as an oxidant at ambient pressure as well as making the MPL robust. Maximum power density of 0.55 W/cm² has been reported.

2.4 KANNAN ET. AL. PAPER ON EFFECT OF CARBON SUBSTRATE OF GDL ON PERFORMANCE OF PEMFC

This paper explains the influence of variable thickness (130, 170, 210, 250, 330 μm) of teflonized non-woven carbon paper substrate developed by Hollingsworth & Vose Co. employed as macro-porous layer on cathode sides at 80 °C using H₂/air as well as H₂/O₂ at different RH conditions on PEMFC performance [31]. Homogenous carbon slurry

consisted of 75 wt.% PB and 25 wt.% VGCF with 25 wt.% PTFE in isopropyl alcohol along with a dispersion agent, Novec-7300 (1 ml for 1 g of carbon). This carbon slurry was coated on the carbon paper substrate using Easycoater equipment (EC26, Coatema) with velocity of 3 m min^{-1} by single pass achieving carbon loading between $2.6\text{-}3 \text{ mg cm}^{-2}$. Although, thinner GDLs should generally be better performers due to shorter path for gas diffusion however Kannan et al. found that thinner GDL with lower porosity cannot provide continuous oxygen supply when the oxidant is air. Thus, they found that $330 \mu\text{m}$ thick substrate having GDL pore volume of 103 cc g^{-1} outperformed $170 \mu\text{m}$ thick substrate having GDL pore volume of 38 cc g^{-1} at all RH conditions (60-100%) using H_2/air as well as H_2/O_2 . An important observation by the authors is significant improvement in fuel cell performance in case of air as well as O_2 as well as homogeneity in surface morphology with the use of dispersing agent (Novec-7300).

2.5 KANNAN ET. AL. PAPER ON WIRE ROD COATING PROCESS OF GAS DIFFUSION LAYER FOR PEMFCS

Kannan et al. [36] employed wire wound rods and an in-house motorized setup for mass fabrication of MPL on non-woven carbon paper substrate by a single pass. They also performed ex-situ characterization methods including surface morphology, contact angle and pore size distribution using FESEM, Goniometer and porosimetry for MPL with carbon composition of 75 wt.% PUREBLACK[®] and 25 wt.% VGCF and uniform PTFE composition of 25 wt.% by using wire rod (RDS50). The MPL showed uniform and crack free surface morphology at low magnification. Using water-ethanol (1:1 ratio) the contact angle measurement was about 120 degrees. These authors conducted multiple experiments

for finding pore diameter values of MPL with various compositions of PB and VGCF. The results suggested a systematic increase in pore diameter when VGCF content increased from 10 to 75 wt.% in MPL. It was established that higher amount of VGCF is more beneficial for good performance at higher relative humidity (100% RH) whereas for lower relative humidity (50% RH) higher amount of PUREBLACK® is more beneficial due to smaller pores in the presence of H₂ as fuel and air as an oxidant. They observed that fuel cell performance of wire rod coated GDL was low for low RH conditions. This could be attributed to large pores and variation in carbon loading between 2.5-3 mg cm⁻², that are certain limitations of manufacturing MPL using wire rod coating method.

2.6 LIM ET. AL. PAPER ON EFFECTS OF HYDROPHOBIC POLYMER CONTENT IN GDL ON POWER PERFORMANCE OF A PEM FUEL CELL

It is evident that there is a strong link between an efficient operation of the PEMFC and an optimized GDL characteristics. In this context, Chan Lim and C.Y. Wang [37] investigated the effect of the addition of 10 to 40 wt. % amount of fluorinated ethylene propylene (FEP) content in the carbon paper GDL on the power performance of H₂/air PEMFC. The authors used a wet-proofed commercial carbon papers (Toray 090, E-Tek) on both the anode and the cathode. The catalysts used is a carbon-supported 20 wt. % Platinum/Carbon (E-Tek Inc.) with a commercial Nafion 112 membrane (EW 1100) from Dupont. In addition Chan Lim and C.Y. Wang measured the polarization curves for each amount of the FEP and they characterized the GDL by measuring the water contact angle with a capillary rise method. The authors deduced from the observed values that an amount of 10 wt. % FEP-impregnated cathode GDL provide higher power densities for the

PEMFC, however there has been no optimization technic applied to confirm that the values obtained are the real optimum for PEMFC performance.

2.7 KANNAN ET. AL. PAPER ON DEVELOPMENT OF GDL USING WATER BASED CARBON SLURRY FOR PEMFC

In this research work, GDL was fabricated with carbon slurry dispersed in variable concentration (25, 50 and 100 mM) of anionic water-soluble micelle surfactant namely SDS [16]. The use of surfactant has demonstrated to control particle size and distribution of nanoparticles deposited on carbon support. Furthermore, SDS helps to homogenously disperse carbon nanotubes in water. Kannan and coworkers also compared GDL fabricated with IPA based carbon slurry with water (SDS) based carbon slurry and found the later to have lesser micro-cracks when observed under SEM however the contact angle remains more or less similar for both. Additionally, they observed that rinsing the GDL in water helps to eliminate sodium ion contamination in MEA which decreases the ionic conductivity of Nafion. They also noted that GDL with SDS concentration of 50 mM performed the best for both H₂/air and H₂/O₂ at 90% RH.

2.8 CHO ET. AL. PAPER ON OPTIMIZATION OF GDLs FOR HIGH PERFORMANCE PEMFC EMPLOYING STAINLESS STEEL BIPOLAR PLATES

Eom and Cho authored an article on influence of variable PTFE content (0-30 wt.%) in MPL of GDL for various RH (25 to 100%), cell temperature (65 to 80 °C) and gas pressure (0 to 1 bar) on the cell performance employing stainless-steel bipolar plate (Grade 316L) [38]. They observed stainless-steel bipolar plate to be more hydrophobic compared

to graphite plate over longer cell operation. This investigation would provide valuable insights for making fuel cell vehicle commercially viable. The paper illustrates the effect of variable RH, cell temperature and gas pressure individually and their interaction with each other. The paper demonstrates that increasing the PTFE content leads to decrease in electrical conductivity and gas and water permeation rates of the GDLs. At a low RH of 25% the cell performance increased with increase in PTFE content. The reason for this is maybe due to decrease in porosity and increase in water retention within the MEA. The paper asserted that the cell temperature increase from 65 °C to 80 °C increased the charge transfer resistance, leading to decrease in cell performance. According to Cho and coworkers, high temperature of 80 °C, low RH (25-50%), and low PTFE content (0-10 wt.%) showed low cell performance. Whereas, high PTFE content (20-30 wt.%) displayed high cell performance. However, increase in the gas pressure decreased the charge transfer resistance, leading to increase in fuel cell performance. Experimental results shows that under unpressurized condition, low PTFE content (0-20 wt.%) and full RH of 100% showed best fuel cell performance while under pressurized conditions (1 bar), higher PTFE content (20-30 wt.%) and low RH of 25% showed the best fuel cell performance. Increase in mass transfer due to gas pressure was relatively more than increase in charge transfer due to increase in RH in case of GDL with high PTFE content. On a whole the authors observed under relatively low temperature (65 °C), high RH (100%) and unpressurized condition, the GDL without PTFE exhibited highest fuel cell performance. In contrast, under higher fuel temperatures of 80 °C, lower RH (25%) and 1 bar of gas pressure, the GDL with 30 wt.% PTFE displayed highest fuel cell performance.

2.9 XIA ET. AL. PAPER ON MOF DERIVED BIFUNCTIONAL OXYGEN ELECTROCATALYST

In 2016, Xia et al [39] used ZIF-67 as only precursor, by one step pyrolysis magically turn it into high ORR performance catalyst, in the atmosphere of H₂/Ar 1:9, heating temperature at 700 °C the nitrogen doped carbon nanotube framework (NCNTF) has been detected. In the heat treatment, because of presence of hydrogen gas form a reducing environment that turns the cobalt ion into cobalt particle as catalyst to let carbon and nitrogen to grow NCNT then many NCNT twisted around together form NCNTF. In this process ZIF-67 not only act as C and N source but also provide catalyst and growth template. The electrocatalytically activity of NCNTF was evaluated by the cyclic voltammetry in O₂ saturated KOH solution, a peak at ~0.78V was observed at cathode indicated good ORR activity. The value of charge transfer numbers are in the range from 3.97 to 3.99 for the range of voltage from 0.3 to 0.7 V which are close to the theoretical value of Pt/C 4.00. Furthermore, unlike most non-Pt electrocatalysts, the NCNTFs catalyst also exhibits high ORR activity in 0.5M H₂SO₄ solution, with an onset potential of 0.85V vs RHE. The linearity of the K-L plots and the calculated electron transfer number of 3.88 in acidic solution also confirm the excellent activity of the NCNTFs catalyst. The pyrolysis temperature was studied from 700 °C to 1000 °C however the resultant of higher temperature electrocatalytically activity decreases. The reason for this is maybe due to the low defect density was formed at higher heat treatment temperature. Moreover, N doping can introduce electrocatalytically active sites in C atoms around N atoms, also N doping generated more defects of NCNTF. N content decreases at higher temperature due to the decomposition of nitrogen group at high temperature. Though pyrolysis temperature at 600

°C has showed most N doping content, it gives low electrocatalytic activity, reason of this is the incomplete pyrolysis of ZIF-67. Existence of Co particle anchored inside the NCNT also play an important role towards ORR and encapsulated Co can't be leached away by acid.

This section will explain the standard operating procedure developed to fulfil the fabrication of various components of PEMFC system and fuel cell assembly. This section is divided into two parts

- a) Fabrication of GDL for optimizing the composition of MPL (PB and PTFE) considering 70 °C for 70% RH using air (as expected in the normal weather condition) as an oxidant.
- b) Pt-NCNTFs cathode catalyst using ZIF-67 for PEMFC.

3.1 EXPERIMENTAL PROTOCOL FOR GDL OPTIMIZATION

3.1.1 Gas Diffusion Layer

Non-teflonized non-woven carbon substrate (GD07508G) was developed and supplied by Hollingsworth & Vose Company. Teflon dispersion (LQ-1005-1000EW, 5% wt.) from Ion Power, Inc., Nano-chain PUREBLACK[®] (grade 205-110) carbon from Superior Graphite Co., VGCF from Superior Graphite Co., and SDS (C₁₂H₂₅SO₄Na) from Fisher Scientific were used for slurry preparation. VGCF was mixed with PUREBLACK[®] to provide improved mechanical strength and adhesion of micro-porous layer with the macro-porous layer.

0.5 g of carbon powder (73.16 wt.% Pure black carbon powder and 26.84 wt.% VGCF) was dispersed in 20 ml DI water containing 120mg of SDS by stirring the mixture for 10 mins and then sonicating for 30 min. PTFE (34 wt.%) dispersion was added into the mixture and followed with the magnetic stirring for 10 min. To coat the paper with carbon

slurry and PTFE, a sample of 10 cm x 10 cm was slowly micro-sprayed. The carbon loading on the micro-porous layer was about 3mg cm^{-2} . After coating the micro-porous layer, the GDL samples were dried at room temperature overnight and then placed in the sintering oven at $350\text{ }^{\circ}\text{C}$ for 30min in air. In order to ensure the best uniformity in PTFE content possible, entire 10 cm x 10 cm sample were sintered, and then cut into individual samples from the sintered square. Nevertheless, a PTFE migration was observed during drying: higher amounts of PTFE dried on all the four edges of the paper in comparison with its center. The carbon and PTFE content in the center of the paper was uniform, and it was from this area that samples used in the experiments were cut. GDL sample was washed to remove the SDS impurities by immersing them in warm DI water for 30 min.

Figure 7 shows the process of MPL preparation.

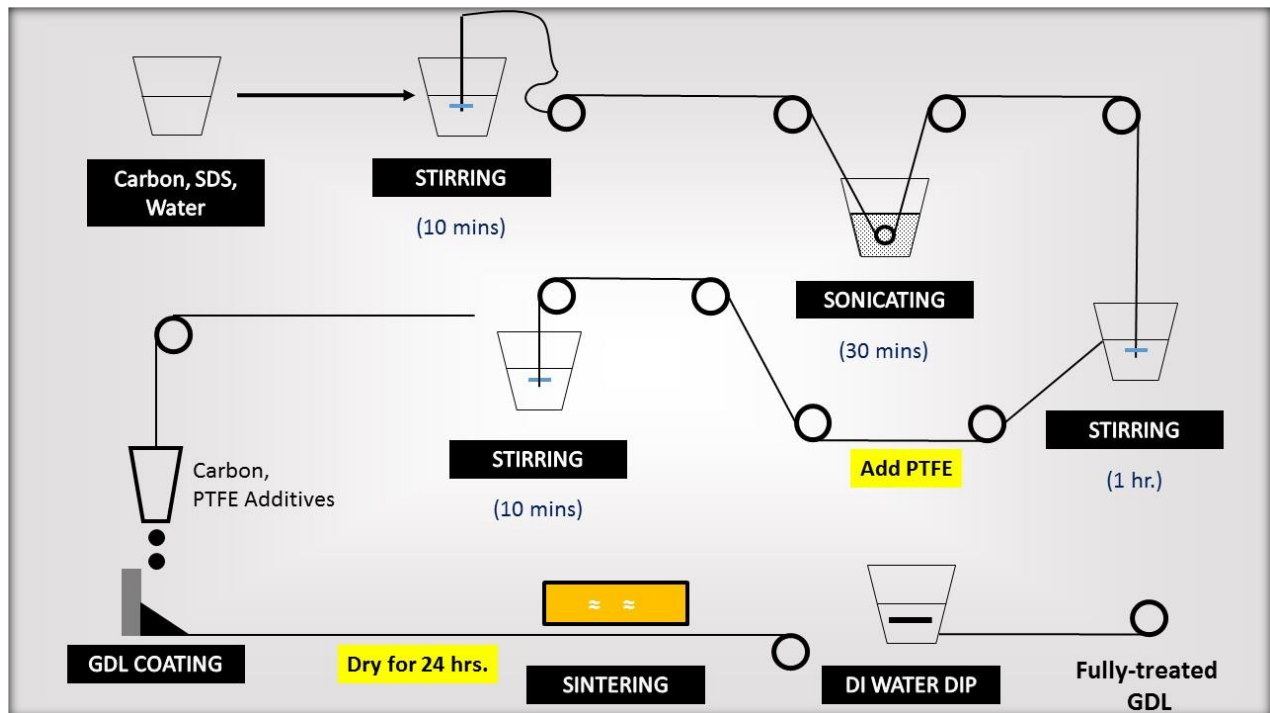


Figure 7 Process of Coating Carbon Paper with Microporous Layer

To improve performance of PEMFCs especially with air as an oxidant, the GDL properties were carefully optimized. In the case of GDL optimization, the complexity of the transport phenomena that occurs and the various material and design of the GDL that exist adding to that the need for a high performance PEMFC, a robust optimization technique is necessary to unlock the link in GDL characteristics and PEMFC performance. The effects of various GDL compositions namely quantity of PB and PTFE, were evaluated using full factorial design of experiments approach.

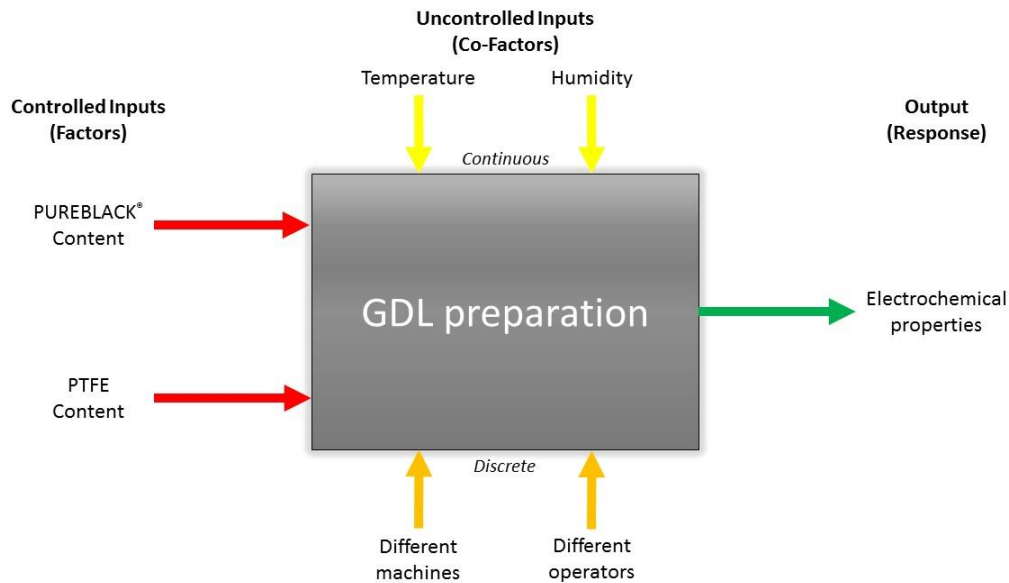


Figure 8 Design of Experiments Approach

Since this is a two-factor factorial i.e. PB content and PTFE content experiment with both design factors at two levels. We have called these levels “low” and “high” and denoted them “-” and “+”, respectively. The objective of this experiment was to determine if adjustments to either of these two factors would increase the maximum power density.

Table 2 Values of Various Individual Parameters at Two Levels

Parameters	Value of variable	
	(-) Low level	(+) High level
A PUREBLACK [®] composition (wt.%)	50	90
B PTFE composition (wt.%)	10	40

It is convenient combinations in standard order (Yate’s order). “A” refers to the effect of factor A, “B” refers to the effect of factor B, and “AB” refers to the AB interaction. The order in which these experiments are performed is random (the order is computer-generated) so that there is no possibility of any bias.

Table 3 2² -Factorial Design: GDL Samples Were Fabricated with Following Different Concentration of PB and PTFE

Run #	Yate’s notation	Parameters	
		A	B
1	(1)	50	10
2	A	90	10
3	B	50	40
4	AB	90	40

3.1.2 Catalyst Coated Membrane

Catalyst-coated membranes (CCM) with 5 cm² active area were fabricated using commercial Pt/C (Tanaka TKK, Japan) catalyst slurry in isopropanol (20 ml for 1 g of electrocatalyst) by the micro-spray method for anode and cathode sides on Nafion[®] membrane (NRE 212, Ion Power Inc., New Castle, DE, USA). The catalyst ink was prepared by dispersing Pt/C in Nafion solution (Ion Power, Inc., LQ-1005-1000 EW, 5% wt.) in order to extend the reaction zone of the catalyst layer and isopropyl alcohol. The membrane was fixed in a home-made fixture to ensure anode and cathode catalyst layers

are exactly on the same area of the membrane. For both anode and cathode, the catalyst loadings were about $0.4 \text{ Pt/C mg cm}^{-2}$, respectively. The MEA was vacuum dried at $60 \text{ }^\circ\text{C}$ for 15 minutes before assembling the electrode in the single cell test cell. Figure 9 shows the process of spraying the CCM. New MEA with same procedure was prepared each time for testing GDL with variable PB and PTFE content.



Figure 9 CCM Micro-Spray Method

3.1.3 Fuel Cell Assembly and Testing

The MEA was assembled by sandwiching inside a single test cell (Fuel Cell Technologies Inc, Albuquerque, NM, USA) along with the GDLs on both sides. Gas sealing was achieved using silicone coated fabric gaskets (Product # CF1007, Saint-Gobain Performance Plastics, USA) and with a uniform torque of 0.45 Nm to seal the single stack test cell. The single stack fuel cell performance was evaluated at 70 °C with various relative humidity (60%, 70%, 80%, and 90% RH) conditions and ambient pressure with H₂/O₂ and H₂/air by using Greenlight Test Station (G50 Fuel Cell System, Hydrogenics, Vancouver, Canada) with fixed flow rates of 200 SCCM on the anode side (H₂) and 300 SCCM on the cathode side (O₂ or air). But since for research only single cell stack fuel cell performance was only emphasized for 70 °C with 70% RH conditions and ambient pressure with H₂/air.

The Greenlight Test Station (G50 Fuel Cell System, Hydrogenics, and Vancouver, Canada) is shown in *Figure 10*. Test scripts were employed for the fuel cell tests. It cycled between 0 to 14 Amp.



Figure 10 Greenlight Test Station (G50 Fuel Cell System, Hydrogenics, and Vancouver, Canada)

3.2 EXPERIMENTAL PROTOCOL FOR PT-NCNTFS CATHODE CATALYST USING ZIF-67

3.2.1 Gas Diffusion Layer

Non-teflonized non-woven carbon paper (GD07508G, Hollingsworth & Vose Company) was used as a substrate for fabricating gas diffusion layers (GDLs). Nano-chain PUREBLACK® carbon (grade 205-110) from Superior Graphite Co., VGCF from Showa Denka, Teflon dispersion (TE-3859) from DuPont Fluoroproducts and SDS ($C_{12}H_{25}SO_4Na$) from Fisher Scientific were used for carbon slurry preparation. 0.5 g of carbon powder (73.16 wt.% Pure black carbon powder and 26.84 wt.% VGCF) was dispersed in 8 ml DI water containing 120 mg of SDS by stirring the mixture for 10 min and sonicated for 30 min. PTFE (34 wt.%) dispersion was added into the mixture and

followed with the magnetic stirring for 10 min. The carbon slurry (micro-porous layer) was coated onto the non-woven carbon paper substrates using Easycoater equipment (EC26, Coatema) at 3 m per min speed. After coating the micro-porous layer, the GDL samples were dried at room temperature overnight followed by sintering at 350 °C for 30 min in air. GDL sample was washed to remove the SDS impurities by immersing in warm DI water for 30 min. The carbon loading on the micro-porous layer was about 3 mg cm⁻², controlled by the wire thickness on the wire rod.



Figure 11 Easycoater Equipment (EC26, Coatema) Used for Coating GDL

3.2.2 Catalyst Coated Membrane

3.2.2.1 Synthesis of ZIF-67 Particles

ZIF-67 samples were synthesized as described in the published literature [39]. In a typical synthesis, 2-methylimidazole (1.97 g) was dissolved in a mixed solution of 20 ml of methanol and 20 ml of ethanol. $\text{Co}(\text{NO}_3)_2 \cdot 6\text{H}_2\text{O}$ (1.746 g) was dissolved in another mixed solution of 20 ml of methanol and 20 ml of ethanol. The above two solutions were then mixed under continuous stirring for few minutes and held for 20 h at room temperature. The purple precipitate was collected by centrifuging the solution, washed in ethanol several times and dried at 80 °C overnight. The flowchart in *Figure 12* provides the process steps sequentially.

3.2.2.2 Synthesis of Pt-NCNTFs

The ZIF-67 particles were soaked with $\text{H}_2\text{PtCl}_6 \cdot 6\text{H}_2\text{O}$ solution (5 wt % solution in DI water) and the resulting material was dried at 80 °C for 1h. The dried powder was heated at 350 °C for 1.5 h then raised to 700 °C at a ramp rate of 2 °C per minute and pyrolyzed for 3.5 h under flowing Ar/H₂ (90% / 10% in volume ratio) atmosphere (see *Figure 12*). The as-prepared black powder product after cooling down to room temperature naturally was treated in 0.5M H₂SO₄ solution for 6 h. The resulting sample was collected by centrifugation, repeatedly washed with DI water, and then dried at 80 °C. NCNTFs were synthesized by following same protocol without adding Pt precursor. The synthesis process reported here used only single precursor as carbon, nitrogen and Co source.

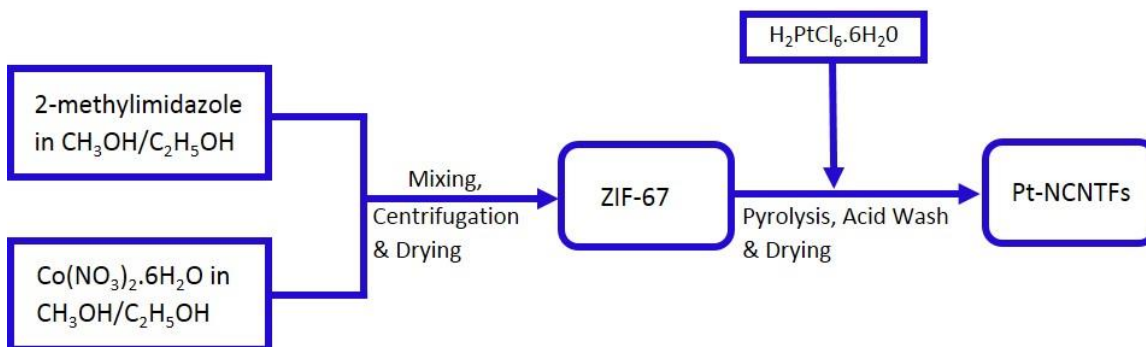


Figure 12 Synthesis of Pt-NCNTFs Using ZIF-67

For PEMFC single cell tests, membrane electrode assemblies (MEAs) with active area of 5.0 cm^2 were fabricated as described below. Commercial Pt/C (Tanaka TKK, Japan) and the Pt-NCNTF were used as anode and cathode catalysts, respectively. The cathode catalyst ink was prepared by dispersing Pt-NCNTFs (or Pt/C for anode) in Nafion solution (Ion Power, Inc., LQ-1005-1000 EW, 5% wt.) and isopropyl alcohol. The catalyst coated membrane (CCM) was fabricated coating the catalyst ink by micro-spray method on Nafion-212 (Ion Power Inc., USA) membrane and vacuum-dried at $70 \text{ }^\circ\text{C}$. The catalyst loading was 0.2 and 0.12 mg cm^{-2} on the anode and cathode sides of the CCM, respectively.

3.2.3 Fuel Cell Assembly and Testing

The MEAs were assembled by sandwiching the CCM with the gas diffusion layers on both sides in the PEMFC test cell (Fuel Cell Technologies Inc., USA) of the CCM. Silicone coated fabric (Product # CF1007, Saint-Gobain Performance Plastics, USA) gasket used and the cell was tightened with a uniform torque of 0.45 Nm . Single cell fuel

cell performance was evaluated using Greenlight Test Station (G50 Fuel Cell Test Station, Hydrogenics, Canada) at 50, 60 and, 70 °C with H₂/O₂ at ambient pressure by galvanostatic polarization. The relative humidity of the reactant gases was maintained at 100 % by controlling the humidity bottle temperatures (both at 400 SCCM, respectively).

4 RESULTS AND DISCUSSION

4.1 GDL OPTIMIZATION

Since the general aim of our research is related to the improvement of fuel cells performance, it has been decided to conduct some performance tests (polarization curves) in various operating conditions in order to show what was the actual effect of the compositions of PB and PTFE on the performances.

Figure 13 shows the PEM fuel cell performance of the MEAs with commercial Pt/C catalysts using H₂ and Air at temperatures of 70 °C and 70 % RH for different concentration of PB and PTFE used in GDL using Greenlight Test Station (G50 Fuel Cell System, Hydrogenics, Vancouver, Canada) with fixed flow rates of 200 SCCM on the anode side (high purity H₂, 99.99%) and 300 SCCM on the cathode side (Air). It is very encouraging to observe that the carbon loading on the micro-porous layer was about 3mg cm⁻² for all the combination of content of PB and PTFE showed a peak power density of 440 mW per cm² at 70 °C with H₂ and Air gases at ambient pressure at 70 % RH.

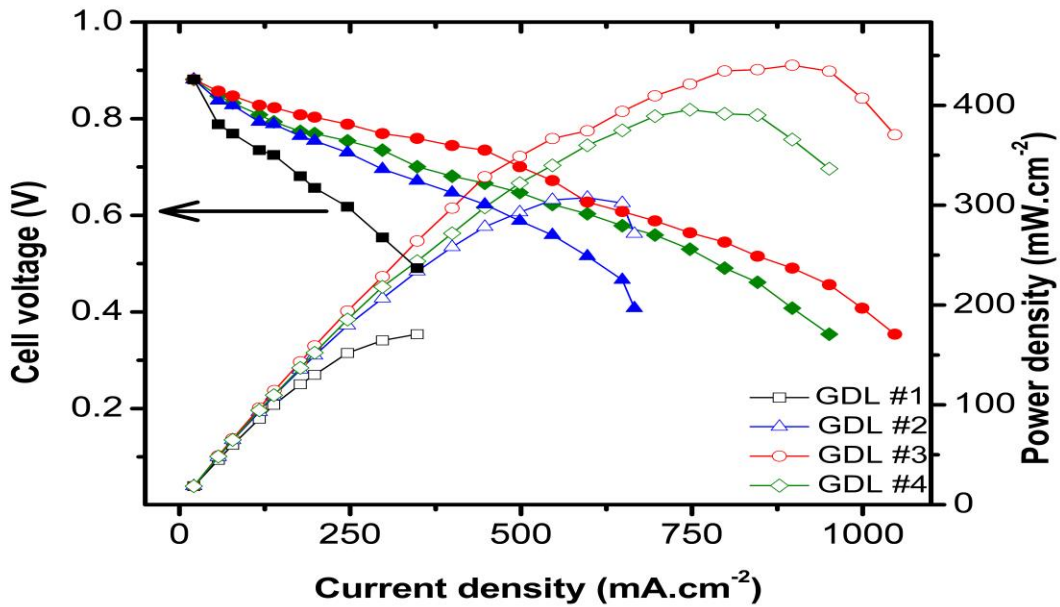


Figure 13 Fuel Cell Performance Using Various Content of PB and PTFE in GDL at 70 °C with H₂ and Air Gases, 70 % RH. The Open Symbols Are the Power Density Values

Table 4 Fuel Cell Performance Data of MEA with Various GDL Compositions

GDL Sample#	Yate's notation	Parameters		Max. power density (mW.cm ⁻²)
		A	B	
1	(1)	50	10	171
2	A	90	10	308
3	B	50	40	440
4	AB	90	40	396

Table 4 compares results of various trials, together with Yates analysis for all the GDL samples with different concentrations of PB and PTFE. It was determined and achieved that GDL sample #3 obtained highest power peak density.

In order to obtain optimum fuel cell performance, a parameter must be shifted from its average from its average value to higher value for a positive effect and to lower value for a negative effect, as dictated by Yate's analysis. Parameter A as well B has a positive mean-

effect value of 48.22 and 182.94 respectively and hence to reach the optimum its value must be shifted to its upper limit.

Keeping the above consideration in view, a total of two typical GDL were fabricated with the values of parameters A and B give in *Table 5*

Table 5 Final Design of GDL

Optimized GDL#	Parameters		Max. power density (mW.cm^{-2})
	A	B	
1	71.58	29.5	415.70
2	73.16	34	486.95

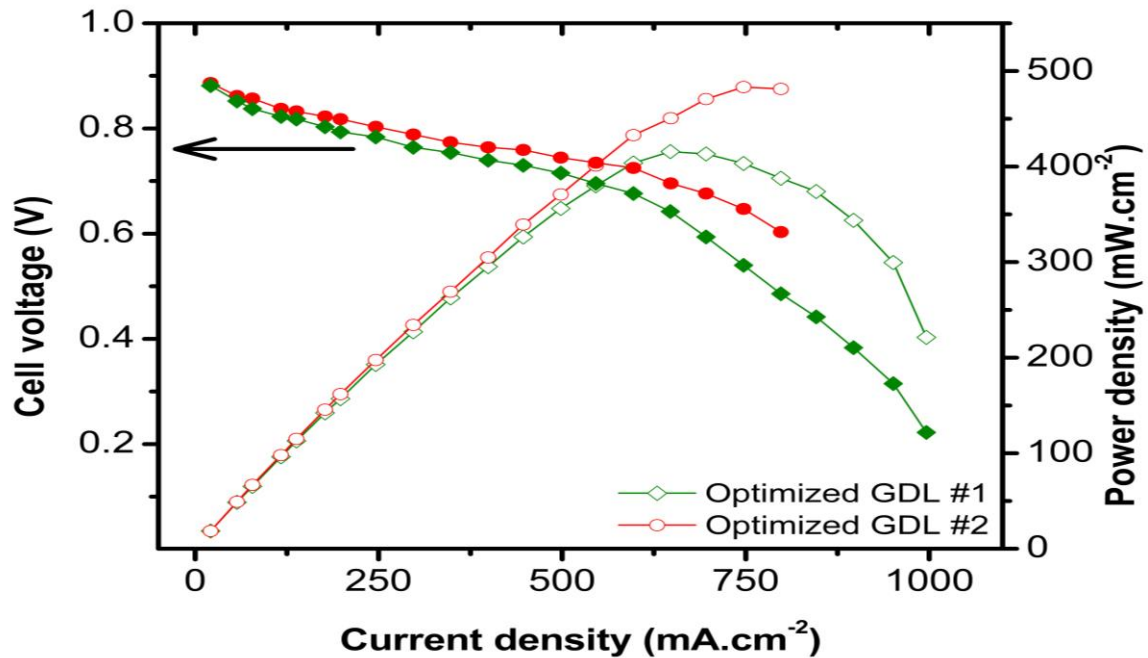


Figure 14 Fuel Cell Performance of Optimized GDL at 70 °C with H₂ and Air Gases, 70 % RH. The Open Symbols Are the Power Density Values

The pore diameter, pore size distribution and pore volume of various GDL samples were measured by Hg porosimeter (PoreMaster-60 GT, Quantachrome Instruments, Boynton Beach, FL). The pore size distributions were calculated from the mercury intrusion data by applying the Washburn equation.

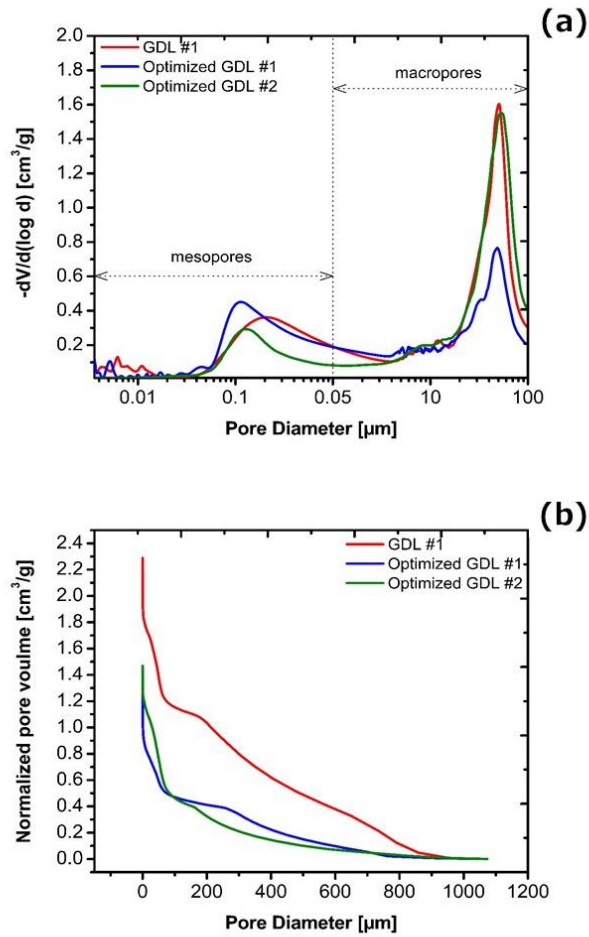


Figure 15 (a) Specific and (b) Cumulative Pore-Size Distribution of Diffusion Layer from Mercury-Intrusion Porosimetry Measurements

The pore size distribution data for various GDL are shown on *Figure 15*. Even though the pore sizes of GDL sample #1 and optimized GDL#2 are close to each other, there is a reduction of pore size for the optimized GDL #1. There is a significant decrease in volume of smaller pore at $\sim 0.1 \mu\text{m}$ observed for GDL sample#1 and optimized GDL#2, along with an increase in volume of the larger pore at $\sim 50 \mu\text{m}$. It is observed that the GDLs fabricated with water based slurries have majority of the pores in the region of $\sim 50 \mu\text{m}$. In order for optimum gas and water transport of the GDLs, carbon slurry permeating into the macro-porous carbon paper has to be prevented. GDL possesses many macro-holes and it enables more gas to transport through the GDL as pressure increase. The carbon slurry permeation into the macro-porous layer is extremely low for the water based slurry due to its hydrophobic characteristics.

Apparently, the range of pore-size is broadly distributed between 0.004 and $1000 \mu\text{m}$, but small pores with the diameters less than $20 \mu\text{m}$ occupy 80% of the total pore volume.

The wetting characteristics (contact angle) of the GDLs were measured by Raméhart Advanced Automated Goniometer using water. *Figure 16* shows the influence of the PTFE content in the MPL on the contact angle. When the PTFE content increases from 5 to 40 wt.%, the contact angle is extended from 119° to 142° , which enhances the hydrophobic properties of the GDL.

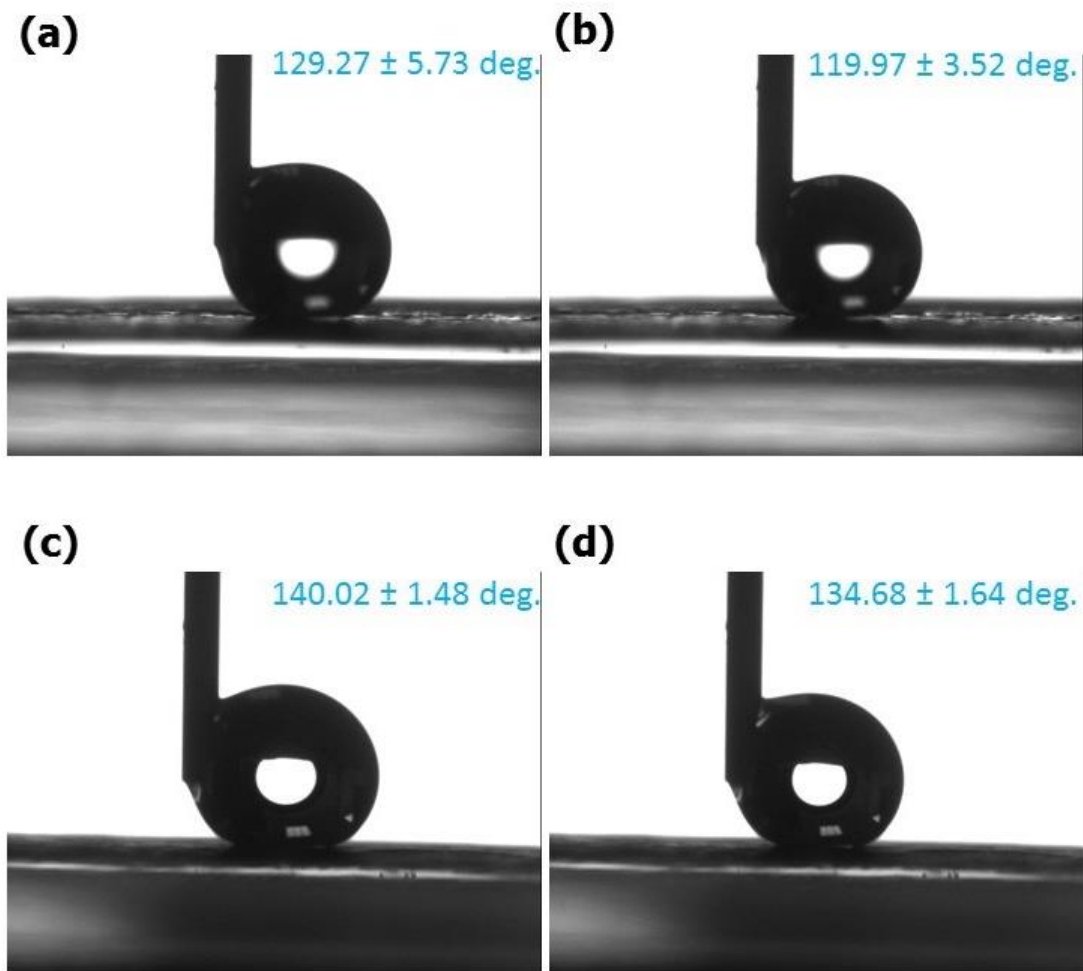


Figure 16 Contact Angle Images of (a) GDL#1 (b) GDL#2 (c) GDL#3 (d) GDL#4

The angle measured by the tangent line for the optimized GDLs are about 155° .

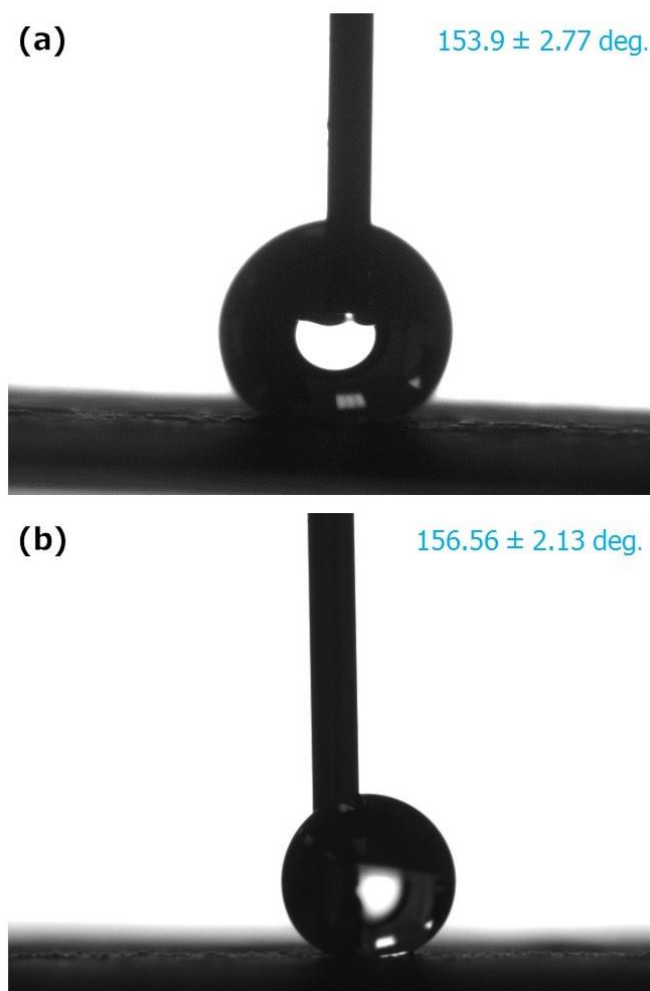


Figure 17 Wetting Angle Images of (a) Optimized GDL#1 (b) Optimized GDL#2

The morphology and structure of the GDL were characterized by Scanning Electron Microscopy (SEM, Hitachi S-3500 N). The SEM micrographs GDLs showed crack free microporous layer favoring uniform gas distribution. The nano-fibrous carbon imparts structural integrity of the micro-porous layer to the GDL substrate.

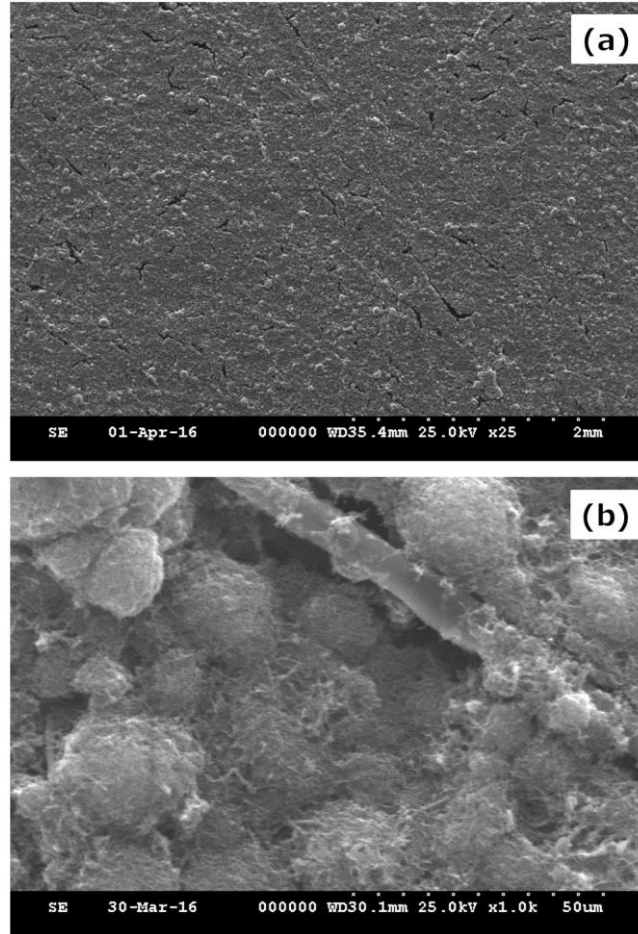


Figure 18 Scanning Electron Micrographs of Surface of Optimized Diffusion Layer #2 at (a) 25x (b) 1000x

The thermal conductivity of the hydrophobed paper was measured by sandwiching samples between two carefully aligned copper electrodes, and thermal conductivity was 0.44 W/mk with total error of 11.84% when measured at 70 °C and pressure of 1.4 Mpa. The GDL's were stacked together for this test and each measured 0.007 inches thick.

4.2 PT-NCNTFS CATHODE CATALYST USING ZIF-67

The surface morphology as well as the physical dimension of the NCNTFs and Pt-NCNTFs cathode catalysts as examined under SEM and TEM are shown in *Figure 19* (a and c) and *Figure 19* (b and d), respectively. As can be seen clearly from the SEM images, the carbon nanotubes are grown on the surface of ZIF-67, which is slightly different from the published literature [40]. The possible reason for the growth of carbon nanotubes is due to the more reducing environment under flowing Ar gas with 10 % H₂ during the pyrolysis, similar to a CVD process. As evident from the TEM image shown in *Figure 19 c*, the presence of well-defined multiwall carbon nanotubes is confirmed, as observed in the surface examination by SEM. The darker spot located at upper right is Co particle as measured by EDS analysis with ~15 nm in diameter. As seen in *Figure 19 d*, the average Pt particle sizes are in the range of 7-10 nm, which could lead to fairly high performance and longevity. The catalyst particles are in the range of 4 to 8 nm yielding good performance and improved durability [41].

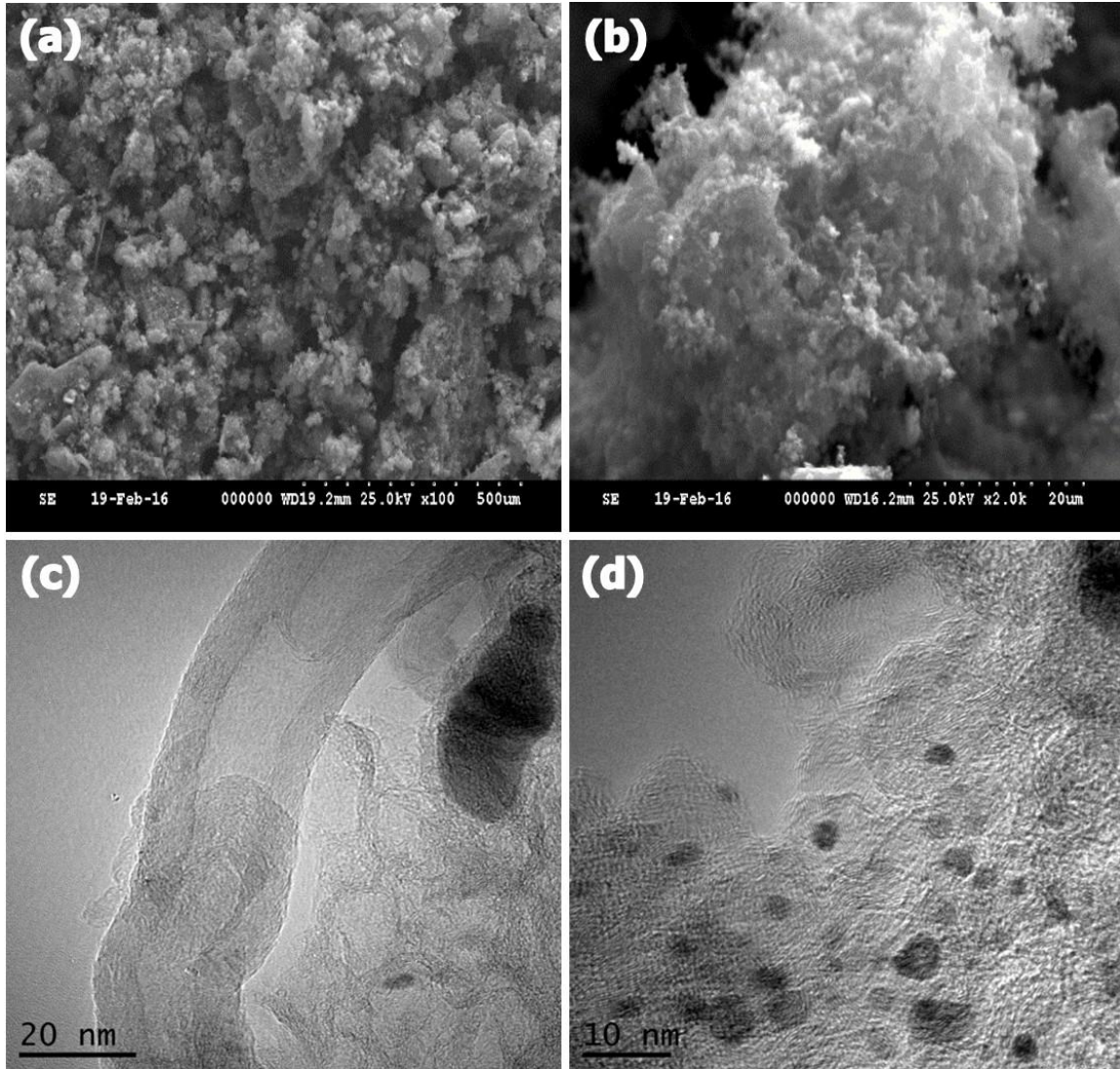


Figure 19 Scanning Electron Micrographs of (a,b) Pt-NCNTFs, and Transmission Electron Micrographs of (c) NCNTFs and (d) Pt-NCNTFs

In addition, graphitic lattice fringes (with 0.34 nm) are also evidenced for providing superior conducting network as well as electrochemical stability. XRD patterns for NCNTFs and Pt-NCNTFs are given in *Figure 20*. As clearly observed, both the NCNTFs

and Pt-NCNTFs show the presence of graphitic carbon at 2Θ value of ~ 26.3 (hkl value: 002), confirming the graphitized CNTs under TEM examination. Other 3 diffraction peaks in the NCNTFs (*Figure 20 a*) are identified as Co (111), Co (200) and Co (220) planes at the 2Θ values of 44.36, 51.67 and 75.98, respectively. In the case of Pt-NCNTFs, the presence of Pt-Co alloy is identified and is expected to exhibit enhanced electrochemical performance towards ORR [42]. Based on the lattice parameters of Pt (3.92 Å) and Co (3.53 Å), the composition of the Pt-NCNTFs (3.86 Å) is estimated to be 84 - 16 atomic wt. % Pt-Co alloy using Vegard's law [43]. From the Scherrer Equation the average crystallite size was calculated by Full width at half maximum (FWHM), for the Pt-NCNTFs as 10.5 nm which is nearly identical to the values estimated from TEM images.

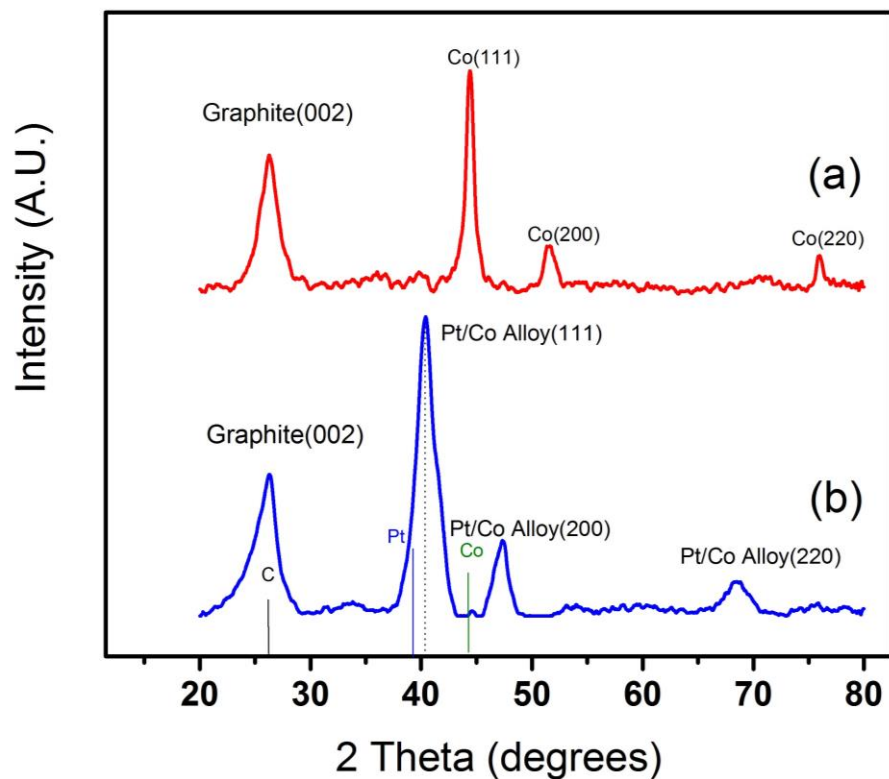


Figure 20 X-Ray Diffractograms of (a) NCNTFs and (b) Pt-NCNTFs

Figure 21 shows the PEM fuel cell performance of the MEAs with Pt-NCNTFs cathode and commercial Pt/C anode catalysts using H₂ and O₂ at various temperatures up to 70 °C. It is very encouraging to observe that the cathode with extremely low loading of 0.12 mg Pt per cm² showed a peak power density of 630 mW per cm² at 70 °C with H₂ and O₂ gases at ambient pressure at 100 % RH. Further evaluation of the catalysts under various operating conditions as well as durability is in progress.

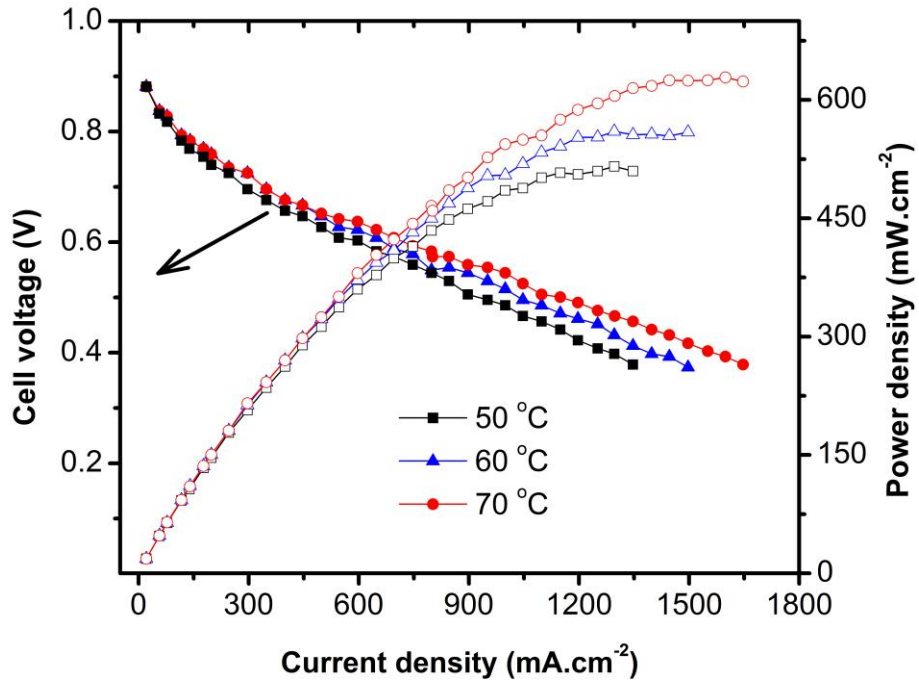


Figure 21 Fuel Cell Performance using Pt-NCNTFs Cathode Catalysts at Various Temperatures with H₂ and O₂ gases, 100 % RH. The Open Symbols are the Power Density Values

The main conclusion of this work is that enhancing the knowledge on the materials properties is of major interest to better understand and increase the performance. The best performance with approximately 490 mA/cm^2 at 650 mV was obtained, when the GDL was fabricated by spraying ink of compositions as follows: 0.5 g of carbon powder ($73.16 \text{ wt.}\%$ Pure black carbon powder and $26.84 \text{ wt.}\%$ VGCF) dispersed in $34 \text{ wt.}\%$ PTFE, maintaining a constant composition for the catalytic layer with a Pt-loading of 0.4 mg cm^{-2} .

Pt nanoparticles of size 10 nm were supported on nitrogen doped carbon nanotubes framework prepared from pyrolysis of ZIF-67 at $700 \text{ }^\circ\text{C}$ in an Ar/H_2 environment. ZIF-67 served as single source for Co, C and N. The MEA with Pt-NCNFs nanocatalyst showed excellent PEMFC performance with a peak power density of 630 mW.cm^{-2} using Nafion-212 membrane at $70 \text{ }^\circ\text{C}$ with H_2 and O_2 gases at ambient operating pressure. The remarkable fuel cell performance with lower Pt loading towards ORR could be attributed to the synergistic effect from Pt, Co, Pt-Co alloy, nitrogen and carbon nanotubes framework.

Future scope can be as follows:

- a) Automotive FC must withstand load cycling and freeze-thaw environmental swings with an acceptable level of degradation from the beginning-of-life (BOL) performance over a life time of 5500 h ($\sim 165,000 \text{ miles}$ at 30 mph)

- b) Mass production methods are the key components to commercial viability of FC systems
- c) In addition, the thesis work done can be evaluated under various RH conditions using H₂/O₂ and H₂/Air for EIS.

- [1] U. E. I. Administration, "Petroleum & Other Liquids," www.eia.gov, 2012.
- [2] U. E. P. Agency, "Inventory of U.S. Greenhouse Gas Emissions and Sinks," www.epa.gov, 1990-2013.
- [3] S. Solomon, D. Qin, M. Manning, Z. Chen, M. Marquis, K. B. Averyt, *et al.*, "Climate Change 2007: The Physical Science Basis. Contribution of Working Group I to the Fourth Assessment Report of the Intergovernmental Panel on Climate Change," Cambridge University Press, New York 2007.
- [4] F. Barbir, *PEM fuel cells: theory and practice*. San Diego , California, USA: Elsevier Academic Press, 2005.
- [5] S. Srinivasan, O. Velez, A. Parthasarathy, D. Manko, and A. Appleby, "High energy efficiency and high power density proton exchange membrane fuel cells — electrode kinetics and mass transport," *Journal of Power Sources*, vol. 36, pp. 299-320, 1991.
- [6] O. S. Burheim, H. Su, S. Pasupathi, J. G. Pharoah, and B. G. Pollet, "Thermal conductivity and temperature profiles of the micro porous layers used for the polymer electrolyte membrane fuel cell," *International Journal of Hydrogen Energy*, vol. 38, pp. 8437-8447, 2013.
- [7] U. Pasaogullari and C. Y. Wang, "Two-phase transport and the role of micro-porous layer in polymer electrolyte fuel cells," *Electrochimica Acta*, vol. 49, pp. 4359-4369, 2004.
- [8] A. M. Kannan, L. Cindrella, and L. Munukutla, "Functionally graded nano-porous gas diffusion layer for proton exchange membrane fuel cells under low relative humidity conditions," *Electrochimica Acta*, vol. 53, pp. 2416-2422, 2008.
- [9] Z. Qi and A. Kaufman, "Low Pt loading high performance cathodes for PEM fuel cells," *Journal of Power Sources*, vol. 113, pp. 37-43, 2003.

- [10] L. R. Jordan, A. K. Shukla, T. Behrsing, N. R. Avery, B. C. Muddle, and M. Forsyth, "Diffusion layer parameters influencing optimal fuel cell performance," *Journal of Power Sources*, vol. 86, pp. 250-254, 2000.
- [11] C. S. Kong, D. Y. Kim, T. H. Lee, H. K. Lee, and Y. G. Shul, "Influence of pore-size distribution of diffusion layer on mass-transport problems of proton exchange membrane fuel cells," *Journal of Power Sources*, vol. 108, pp. 185-191, 2002.
- [12] Z. Zhan, J. Xiao, Y. Zhang, M. Pan, and R. Yuan, "Gas diffusion through differently structured gas diffusion layers of PEM fuel cells," *International Journal of Hydrogen Energy*, vol. 32, pp. 4443-4451, 2007.
- [13] D. P. Wilkinson, *Proton exchange membrane fuel cells: materials properties and performance*. Boca Raton, FL: CRC Press/Taylor & Francis, 2010.
- [14] M. F. Mathias, J. Roth, J. Fleming, and W. Lehnert, *Handbook of Fuel Cells Fundamentals Technology and Applications*: John Wiley and Sons, Ltd, 2010.
- [15] C. Richard, F. Balavoine, P. Schultz, T. W. Ebbesen, and C. Mioskowski, "Supramolecular Self-Assembly of Lipid Derivatives on Carbon Nanotubes," *Science*, vol. 300, pp. 775-778, 2003.
- [16] J. F. Lin, X. Liu, A. Adame, R. Villacorta, J. Wertz, R. Ahmad, *et al.*, "Development of gas diffusion layer using water based carbon slurry for proton exchange membrane fuel cells," *Electrochimica Acta*, vol. 56, pp. 1591-1596, 2011.
- [17] J. A. Kerres, "Development of ionomer membranes for fuel cells," *Journal of Membrane Science*, vol. 185, pp. 3-27, 2001.
- [18] J. Suntivich, H. A. Gasteiger, N. Yabuuchi, H. Nakanishi, J. B. Goodenough, and Y. Shao-Horn, "Design principles for oxygen-reduction activity on perovskite oxide catalysts for fuel cells and metal-air batteries," *Nature chemistry*, vol. 3, pp. 546-550, 2011.
- [19] P. G. Bruce, S. A. Freunberger, L. J. Hardwick, and J. Tarascon, "Li-O₂ and Li-S batteries with high energy storage," *Nature Materials*, vol. 11, pp. 19-29, 2012.

- [20] R. Borup, "Scientific Aspects of Polymer Electrolyte Fuel Cell Durability and Degradation," *ChemInform*, vol. 38, 2007.
- [21] J. C. Meier, I. Katsounaros, C. Galeano, H. J. Bongard, A. A. Topalov, A. Kostka, *et al.*, "Stability investigations of electrocatalysts on the nanoscale," vol. 5, pp. 9319-9333, 2012.
- [22] T. Palaniselvam, B. P. Biswal, R. Banerjee, and S. Kurungot, "Zeolitic imidazolate framework (ZIF)-derived, hollow-core, nitrogen-doped carbon nanostructures for oxygen-reduction reactions in PEFCs," *Chemistry (Weinheim an der Bergstrasse, Germany)*, vol. 19, pp. 9335-9342, 2013.
- [23] P. Zhang, F. Sun, Z. Xiang, Z. Shen, J. Yun, and D. Cao, "ZIF-derived in situ nitrogen-doped porous carbons as efficient metal-free electrocatalysts for oxygen reduction reaction," vol. 7, pp. 442-45, 2013.
- [24] H. L. Jiang, B. Liu, Y. Q. Lan, K. Kuratani, T. Akita, H. Shioyama, *et al.*, "From metal-organic framework to nanoporous carbon: toward a very high surface area and hydrogen uptake," *Journal of the American Chemical Society*, vol. 133, p. 11854, 2011.
- [25] Z. S. Wu, L. Chen, J. Liu, K. Parvez, H. Liang, J. Shu, *et al.*, "High - Performance Electrocatalysts for Oxygen Reduction Derived from Cobalt Porphyrin - Based Conjugated Mesoporous Polymers," *Advanced Materials*, vol. 26, pp. 1450-1455, 2014.
- [26] D. Zhao, J. L. Shui, L. R. Grabstanowicz, C. Chen, S. M. Commet, T. Xu, *et al.*, "Highly Efficient Non - Precious Metal Electrocatalysts Prepared from One - Pot Synthesized Zeolitic Imidazolate Frameworks," *Advanced Materials*, vol. 26, pp. 1093-1097, 2014.
- [27] D. Zhao, J. L. Shui, C. Chen, X. Chen, B. M. Repogle, D. Wang, *et al.*, "Iron imidazolate framework as precursor for electrocatalysts in polymer electrolyte membrane fuel cells," vol. 3, pp. 32-325, 2012.

- [28] W. Zhang, Z. Y. Wu, H. L. Jiang, and S. H. Yu, "Nanowire-directed templating synthesis of metal-organic framework nanofibers and their derived porous doped carbon nanofibers for enhanced electrocatalysis," *Journal of the American Chemical Society* vol. 136, p. 14385, 2014.
- [29] P. Su, H. Xiao, J. Zhao, Y. Yao, Z. Shao, C. Li, *et al.*, "Nitrogen-doped carbon nanotubes derived from Zn-Fe-ZIF nanospheres and their application as efficient oxygen reduction electrocatalysts with in situ generated iron species," vol. 4, pp. 2941-2946, 2013.
- [30] J. M. Morgan and R. Datta, "Understanding the gas diffusion layer in proton exchange membrane fuel cells. I. How its structural characteristics affect diffusion and performance," *Journal of Power Sources*, vol. 251, pp. 269-278, 2014.
- [31] J. F. Lin, J. Wertz, R. Ahmad, M. Thommes, and A. M. Kannan, "Effect of carbon paper substrate of the gas diffusion layer on the performance of proton exchange membrane fuel cell," *Electrochimica Acta*, vol. 55, pp. 2746-2751, 2010.
- [32] A. Arvay, E. Yli-Rantala, C. H. Liu, X. H. Peng, P. Koski, L. Cindrella, *et al.*, "Characterization techniques for gas diffusion layers for proton exchange membrane fuel cells – A review," *Journal of Power Sources*, vol. 213, pp. 317-337, 2012.
- [33] I. Nitta, O. Himanen, and M. Mikkola, "Contact resistance between gas diffusion layer and catalyst layer of PEM fuel cell," *Electrochemistry Communications*, vol. 10, pp. 47-51, 1// 2008.
- [34] D. C. Montgomery, *Design and analysis of experiments* vol. Eighth. Hoboken, NJ: John Wiley & Sons, Inc, 2013.
- [35] A. Kannan, A. Menghal, and I. Barsukov, "Gas diffusion layer using a new type of graphitized nano-carbon PUREBLACK® for proton exchange membrane fuel cells," *Electrochemistry Communications*, vol. 8, pp. 887-891, 2006.
- [36] A. M. Kannan, S. Sadananda, D. Parker, L. Munukutla, J. Wertz, and M. Thommes, "Wire rod coating process of gas diffusion layers fabrication for proton exchange membrane fuel cells," *Journal of Power Sources*, vol. 178, pp. 231-237, 2008.

- [37] C. Lim and C. Y. Wang, "Effects of hydrophobic polymer content in GDL on power performance of a PEM fuel cell," *Electrochimica Acta*, vol. 49, pp. 4149-4156, 2004.
- [38] K. Eom, E. Cho, J. Jang, H.-J. Kim, T.-H. Lim, B. K. Hong, *et al.*, "Optimization of GDLs for high-performance PEMFC employing stainless steel bipolar plates," *International Journal of Hydrogen Energy*, vol. 38, pp. 6249-6260, 2013.
- [39] B. Y. Xia, Y. Yan, N. Li, H. B. Wu, X. W. Lou, and X. Wang, "A metal-organic framework-derived bifunctional oxygen electrocatalyst," *Nature Energy*, vol. 1, p. 15006, 2016.
- [40] S. H. Hsu, C. T. Li, H. T. Chien, R. R. Salunkhe, N. Suzuki, Y. Yamauchi, *et al.*, "Platinum-free counter electrode comprised of metal-organic-framework (MOF)-derived cobalt sulfide nanoparticles for efficient dye-sensitized solar cells (DSSCs)," *Sci Rep*, vol. 4, p. 6983, 2014.
- [41] J. F. Lin, A. Adame, and A. M. Kannan, "Development of Durable Platinum Nanocatalyst on Carbon Nanotubes for Proton Exchange Membrane Fuel Cells," *Journal of The Electrochemical Society*, vol. 157, p. B846, 2010.
- [42] D. Wang, H. L. Xin, R. Hovden, H. Wang, Y. Yu, D. A. Muller, *et al.*, "Structurally ordered intermetallic platinum-cobalt core-shell nanoparticles with enhanced activity and stability as oxygen reduction electrocatalysts," *Nature materials*, vol. 12, p. 81, 2013.
- [43] G.-H. Wang, J. Hilgert, F. H. Richter, F. Wang, H.-J. Bongard, B. Spliethoff, *et al.*, "Platinum-cobalt bimetallic nanoparticles in hollow carbon nanospheres for hydrogenolysis of 5-hydroxymethylfurfural," *Nature materials*, vol. 13, p. 293, 2014.